FACULTY
OF MATHEMATICS
AND PHYSICS
Charles University

Institute of Particle and Nuclear Physics

Multiphonon and shell model approaches to nuclear spectroscopy

František Knapp

HABILITATION THESIS

Prague 2022

First of all, I would like to address my many thanks to my wife and my children, especially for their love, support, and patience. I am also deeply indebted to my parents, who supported me during all my studies. I would like to express my deepest gratitude to my mentors and friends, Nicola Lo Iudice and Jan Kvasil, who introduced me into the fascinating world of atomic nuclei. I am also grateful to all my colleagues I worked with in Prague and Naples.

Contents

Introduction **5**

1 Nuclear collective vibrations **7**
- 1.1 Giant resonances . . . 7
- 1.2 Theoretical modeling of collective states . . . 10
  - 1.2.1 Microscopic models of harmonic vibrations . . . 11
  - 1.2.2 Extensions of RPA . . . 16
- 1.3 Equation of motion phonon method . . . 20
  - 1.3.1 EMPM for even-even systems . . . 20
  - 1.3.2 EMPM for systems with valence particle(hole) . . . 26
  - 1.3.3 Center-of-mass problem in EMPM . . . 30

2 Shell model calculations **35**
- 2.1 Shell model with important sampling . . . 35
- 2.2 Importance truncation in SA-NCSM . . . 36

Conclusion **39**

Bibliography **41**

A EMPM original papers **51**
- A.1 A self-consistent study of multipole response in neutron-rich nuclei using a modified realistic potential . . . 51
- A.2 Upgraded formulation of the nuclear eigenvalue problem in a microscopic multiphonon basis . . . 51
- A.3 Dipole response in ^{132}Sn within a self-consistent multiphonon approach . . . 51
- A.4 Self-consistent quasiparticle formulation of a multiphonon method and its application to the neutron-rich ^{20}O nucleus . . . 52
- A.5 Ground-state correlations within a nonperturbative approach . . . 52
- A.6 Low- and high-energy spectroscopy of ^{17}O and ^{17}F within a microscopic multiphonon approach . . . 52
- A.7 Proper treatment of the Pauli principle in mirror nuclei within the microscopic particle(hole) -phonon scheme . . . 52
- A.8 Removal of the center of mass in nuclei and its effects on ^{4}He . . . 53
- A.9 Spectroscopic properties of ^{4}He within a multiphonon approach . . . 53

B Shell model original papers **55**
- B.1 Matrix diagonalization algorithm and its applicability to the nuclear shell model . . . 55
- B.2 Importance-sampling diagonalization algorithm for large-scale shell model calculations on N = 80 isotones . . . 55
- B.3 Mixed-symmetry states in Te isotopes within a large-scale shell model approach . . . 55
- B.4 Importance basis truncation in the symmetry-adapted no-core shell model . . . 55

List of abbreviations

ChPT	Chiral perturbation theory
CM	Center of mass
EMPM	Equation of motion phonon method
ETFFS	Extended theory of finite Fermi systems
GDR	Giant dipole resonance
IS	Importance sampling
IT-NCSM	Importance-truncated no-core shell model
IVGDR	Isovector giant dipole resonance
HF	Hartree-Fock
HFB	Hartree-Fock-Bogolyubov
IBM	Interacting boson model
NCSM	No-core shell model
ph	particle-hole
np-nh	n-particle n-hole
PDR	Pygmy dipole resonance
QCD	Quantum chromodynamics
qp	quasiparticle
QPM	Quasiparticle phonon model
QTBA	Quasiparticle time blocking approximation
RPA	Random phase approximation
SA-NCSM	Symmetry-adapted no-core shell model
SM	Shell model
TDA	Tamm-Dancoff approximation
UCOM	Unitary Correlation Operator Method

Introduction

Atomic nuclei are fascinating examples of strongly interacting quantum many-body systems. Over more than one hundred years since the discovery of the nucleus by Ernest Rutheford, we have accumulated an enormous amount of theoretical and experimental knowledge about nuclear structure. We have invented many nuclear models, which, in connection with immense progress in experimental techniques, allowed us to get at least a partial insight into a wide variety of nuclear phenomena. Despite the complexity of the computational many-body methods employing state-of-the-art models of internucleonic interactions, our understanding is built on several simple concepts that capture essential features of most nuclei.

In the traditional view, the atomic nucleus is modeled as a self-bound system consisting of strongly interacting point-like nonrelativistic nucleons. Though we deal with many nucleons, it is remarkable that many nuclear properties are driven by the motion of a few individual constituents. That is why microscopic models became pillars of modern nuclear theory. The success of microscopic models would not be possible without incredible progress in computational power, along with the development of numerical algorithms and methods for large-scale diagonalizations of effective nuclear Hamiltonians. Besides the single-particle features, an inherent attribute of all nuclei is the existence of collective excitations, formed as a coherent action of many nucleons. Representative examples are rotations of deformed nuclei and vibrations occurring both in spherical and deformed systems. Since similar types of collective motion are well-known in molecules, it is not surprising that many theoretical concepts used for describing atomic and molecular systems were brought to nuclear physics theory and vice versa. Typical examples are mean-field Hartree-Fock(HF) and Hartree-Fock-Bogolyubov (HFB) methods, density functional theory (DFT), or Random Phase Approximation (RPA).

An indispensable role in our understanding of nuclear spectra is played by the phenomenological collective models of Bohr and Motellsson and the Interacting boson model (IBM) of Arima and Iacchello, which grasp the main aspects of nuclear collective motion by suitably chosen collective degrees of freedom. Altogether, different facets of nuclear structure demonstrate the uniqueness of atomic nuclei as laboratories for studying the quantum many-body problem.

Although we fairly well understand the microscopic origin of collective modes in nuclei, a precise quantitative description of such excitations in medium-heavy and heavy nuclei by employing modern nucleon-nucleon interactions is still missing. Therefore it persists an urgent need to develop novel many-body techniques and approximation schemes that push the limits of present-day approaches toward a unified description of low- and high-energy collective states.

My scientific work represents a little piece contributing to this ongoing, seemingly neverending effort. I was mainly focused on developing microscopic approaches for calculating spectra and collective electromagnetic transitions in spherical nuclei and truncation schemes in shell model calculations. I am a co-author of 27 papers in referred journals and about the same contributions to conference proceedings. The submitted habilitation thesis provides an overview of problems I have worked on and discusses selected results.

Most of the work was done in close collaboration with respected colleagues from

Instituto Nazionale di Fisica Nucleare and Universita di Federico II, which was initiated mainly during my post-doctoral stay in Naples in 2009-2010 and continues until today.

The thesis comprises two parts and appendices with reprints of selected papers. In chapter 1, I explain motivation and basic principles of microscopic methods commonly used to describe collective vibrations. The core of the thesis, section 1.3, introduces the Equation of motion phonon approach (EMPM) for the description of collectivity in spherical closed-shell nuclei and nuclei with one valence particle (hole). This section is supplemented with nine papers attached in Appendix A. I signifficantly contributed to formal development of this novel theoretical approach, as well as to its practical implementation and numerical calculations. The chapter 2, supplemented with four papers in Appendix B, is devoted to methods for truncation of model spaces used in the shell model calculations, which I contributed to durig my post-doc stay in Naples.

The work presented in the thesis was partly supported by the Czech Science Foundation grants P203-13-07117S, P203-16-16772S, and P203-19-14048S and by the Charles University Research Center UNCE/SCI/013.

1. Nuclear collective vibrations

The quantum liquid drop picture of the atomic nucleus readily evokes an image of surface vibrations when the system is excited with an external perturbation. Such vibrations are inherent to spherical and deformed nuclei across the whole mass table. Apart from small amplitude oscillations, manifested as low-lying collective vibrational states of specific angular momenta and parities, excitations corresponding to a large-amplitude motion are well recognized in nuclear spectra. In this chapter, we recapitulate the key quantities used to characterize collective states in atomic nuclei, and further, we give an overview of commonly accepted microscopic models used for their quantitative description.

1.1 Giant resonances

The most prominent examples of collective excitations in nuclei are giant resonances (GR) - large amplitude oscillations of different types (shape, spin, isospin) and multipolarities (monopole, dipole, quadrupole, octupole) which can be invoked by an external perturbation (e. g. photons or charged projectiles). They are formed by a nuclear motion to which many individual nucleons contribute coherently. Giant resonances are manifested as significant, broad humps in the cross sections of specific nuclear reactions and form prominent peaks in nuclear response functions of corresponding types and multipolarities.

Electromagnetic probes play a unique role in the research of nuclear collectivity. Indeed, an enormous amount of experimental and theoretical studies have been devoted to electromagnetic nuclear response functions because they provide clean and unique insight into the internal structure of nuclei.

The collectivity of an individual electromagnetic transition is related to its transition probability. For the transition from an initial state with spin J_i and parity π_i to a final state with spin J_f and parity π_f we define reduced transition probability as

$$B(i \to f, X\lambda) = \frac{|\langle f, J_f, \pi_f || \hat{M}^X_\lambda || i, J_i, \pi_i \rangle|^2}{2J_i + 1}, \tag{1.1}$$

where $\hat{M}^X_\lambda$ is the electromagnetic transition operator, representing photon emission or absorption of electric ($X \equiv E$) or magnetic ($X \equiv M$) type and multipolarity λ[1]. A commonly accepted approximation used in nuclear structure calculations of photoabsorption and γ decay processes is that the electromagnetic field interacts with a system of nonrelativistic point-like nucleons. This simplified picture leads to "standard" expressions for transition operators $\hat{M}^X_\lambda$, which can be found in many textbooks (e. g. [RS80]).

However, the density of nuclear states grows rapidly with increasing excitation energy forbidding thus to identify individual transitions. Therefore it is more convenient to define the strength function

$$S(X\lambda, \omega) = \sum_f B(i \to f, X\lambda)\delta(\omega - \omega_{fi}) \approx \sum_f B(i \to f, X\lambda)\rho_\Delta(\omega - \omega_{fi}), \tag{1.2}$$

---

[1] Alternative definitions of transition probability that use other conventions for the reduced matrix element can be found in the literature.

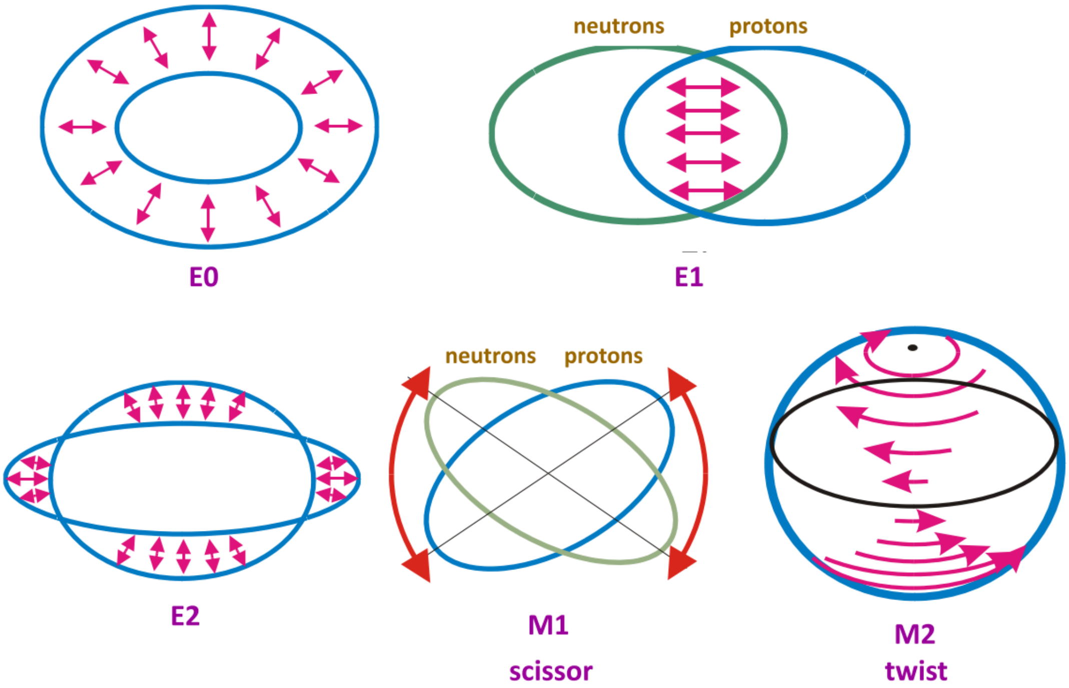

Fig. 1.1: The liquid-drop picture of selected collective modes in nuclei. Different types and multipolarities determine the character of collective motion, e. g., breathing mode (E0), dipole (E1) and quadrupole (E2) oscillations, scissor-like vibrations (M1), or twist mode (M2). Adopted from [Kva22].

where $\omega_{fi} = E_f - E_i$ denotes the excitation energy of a final state.

The δ-function is in calculations often replaced with appropriate smoothing function $\rho_\Delta(\omega - \omega_{fi})$ with finite width Δ, simulating the continuum and the coupling to complex configurations.

The transition matrix elements $\langle f, J_f, \pi_f || \hat{M}^X_\lambda || i, J_i, \pi_i \rangle$, which can be, in principle, calculated within physically relevant (macroscopic or microscopic) nuclear model is directly related to various experimental observables via definition 1.1. For example, the photoabsorption cross section can be calculated by using the expression

$$\sigma(\omega, i \to f) = \frac{8\pi^3 \hbar c \alpha}{e^2} \sum_{\lambda, X=E,M} \frac{k^{2\lambda-1}}{[(2\lambda+1)!!]^2} \frac{\lambda+1}{\lambda} \delta(\omega - \omega_{fi}) B(i \to f, X\lambda), \quad (1.3)$$

where α is the fine structure constant, e is the elementary charge, c is the speed of light, $\hbar$ is the reduced Planck constant, and $k = \frac{\omega}{\hbar c}$ is the wavenumber of the incident photon.

The important attribute of nuclear states is their collectivity. The transition strength can be used as a criterion to determine how collective is a particular state. By using strength function definition 1.2 we can define energy weighted sum within an energy interval $\langle \omega_{min}, \omega_{max} \rangle$ as

$$S^{X\lambda}_{EW}(\omega_{min}, \omega_{max}) = \int_{\omega_{min}}^{\omega_{max}} S(X\lambda, \omega) \omega d\omega. \quad (1.4)$$

The collectivity in the energy interval $\langle \omega_{min}, \omega_{max} \rangle$ is then proportional to the frac-

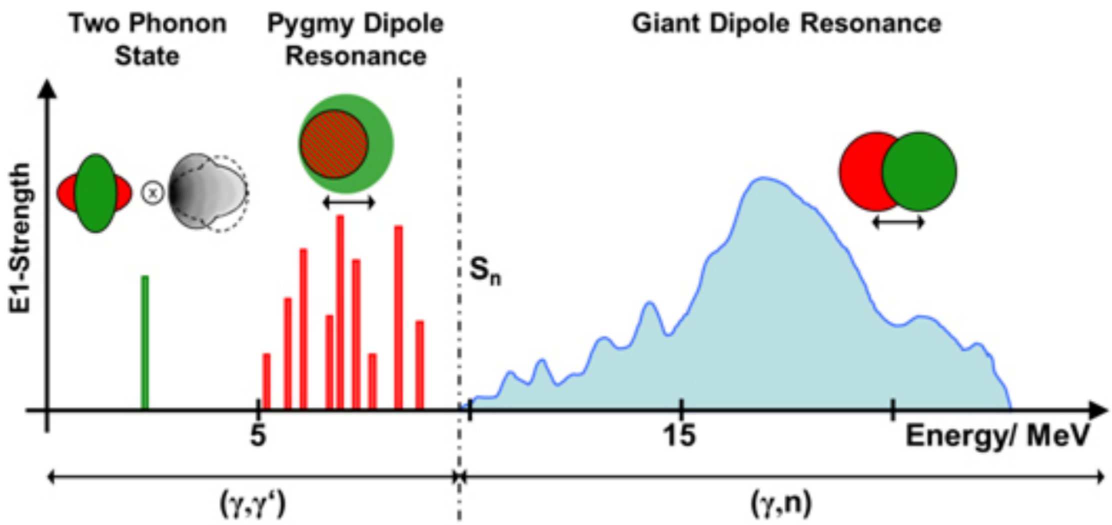

Fig. 1.2: Schematic picture of dipole excitations in spherical nuclei. The high-energy states form IVGDR - collective oscillation of protons against neutrons. Neutron-rich nuclei exhibit another type of dipole collective motion located near the neutron separation energy (S_n), commonly interpreted as neutron skin oscillation against $N = Z$ symmetric core. While GDRs can be reasonably described as harmonic oscillations (one-phonon states), lowest dipole excitations are formed from multiphonon excitations. Adapted from [NuP15].

tion of energy weighted sum exhausted by states in this interval

$$w(\omega_{min}, \omega_{max}) = \frac{S^{X\lambda}_{EW}(\omega_{min}, \omega_{max})}{S^{X\lambda}_{EW}(0, \infty)}. \tag{1.5}$$

Usually, we speak about GR if a significant fraction of the sum rule value $S^{X\lambda}_{EW}(0, \infty)$ (say 50% or more) is exhausted by transitions to states within the region of the resonance. Basic attributes of GRs (position, strength, width) do not depend on details in the microscopic structure of nuclei but rather on their bulk properties and vary smoothly with the nuclear mass.

The mostly studied collective excitations are electric ($X = E$) dipole ($\lambda = 1$) excitations. The high energy part - isovector giant dipole resonance (IVGDR) is observed across the entire nuclide chart, with energy centroid

$$E_x \approx 31.2A^{-\frac{1}{3}} + 20.6A^{-\frac{1}{6}}\text{MeV} \tag{1.6}$$

and width of several MeV [BF75].

Macroscopically, IVGDR can be seen as out-of-phase oscillations of protons against neutrons (see fig. 1.1), as described by Goldhaber-Teller [GT48] and Jensen-Steinwedel [SD50] hydrodynamical models. The E1 contribution to the photoabsorption cross section 1.3 is the most important one, and the IVGDR represents the dominant part of total E1 strength. Therefore dipole approximation is often used in the evaluation of the total photoabsorption cross section,

$$\sigma_{tot} \approx \frac{16\pi^3\alpha}{9e^2}\int_0^\infty \omega S(E1, \omega)d\omega, \tag{1.7}$$

for which Thomas-Reiche-Kunh sum rule provides an estimate (see e. g. [HvdW01])

$$\sigma_{tot} \approx 60\frac{NZ}{A}\text{MeV.mb.} \tag{1.8}$$

Electric dipole excitations have been the subject of theoretical and experimental investigations for decades. However, only recent progress in experimental techniques led to the accumulation of information not only about their gross features but also details about their strength distributions, isospin character, and its relations to neutron skin thickness and nuclear polarizability (for a review, see [BLT19]).

From a theoretical point of view, three main physical mechanisms are responsible for the fine structures and widths of GRs. The first one is the fragmentation of elementary particle-hole (*ph*) excitations (Landau damping), the second one is direct particle emission (escape width), and the third one is the coupling of elementary *ph* states to complex configurations.

A schematic plot of the E1 strength function is shown in fig. 1.2. Apart from the broad IVGDR peak around 20 MeV, in the low energy tail of resonance below a neutron separation energy, we observe transitions forming so-called Pygmy dipole resonance (PDR). The widely accepted macroscopic view of the PDR is that it is a manifestation of neutron skin oscillations against a symmetric ($N = Z$) core. Furthermore, in the low-energy part of the spectrum, states which cannot be interpreted as simple harmonic oscillations but rather as complicated multiphonon excitations are present.

The experimental and theoretical interest in PDR is further motivated by the fact that low-energy dipole strength influences the astrophysical r-process and thus can dramatically impact the abundance of elements formed in the stellar environment [Gor98]. Other types of resonances, widely studied in the last decades with electromagnetic probes, include electric quadrupole (E2), magnetic dipole (M1), and monopole (E0) modes (for a review, see [HvdW01]). Their studies are indispensable not only from a nuclear structure perspective but provide essential inputs for modeling neutron stars, supernovae explosions, and collisions of heavy ions. For example, nuclear matter compressibility can be determined from properties of isoscalar monopole strength functions [SY93].

Let us mention some recent measurements that substantially contributed to understanding the mechanisms responsible for forming collective states and revealed their fine structures in spherical nuclei. Data extracted from (d, p) reactions and the high-energy inelastic scattering of protons became a very powerful tool for the determination of various properties of IVGDR in ^{208}Pb [SHB+20] and ^{120}Sn [WSP+21]. The measurements at forward scattering angles in (p, p') reactions were used to extract information about fine structures of electric and magnetic dipole modes [NCvT19]. Characteristic energy scales present in dipole responses of magic nuclei ^{208}Pb [PFK+14], ^{40,48}Ca [CDF+22] and isoscalar quadrupole responses of ^{40}Ca [UBC+11], ^{28}Si and ^{27}Al [UBC+16] were extracted from data by employing wavelet analysis.

New precise data represent a challenge for the many-body theory because only a comparison with theoretical predictions can shed light on mechanisms responsible for observed fine structures in nuclear response functions.

1.2 Theoretical modeling of collective states

The unified microscopic theory of the atomic nucleus with powerful predictive power is an unfulfilled dream of several generations of nuclear physicists. The well-known obstacle which prohibits straightforward *ab initio* modeling of nuclei from the underlying theory of strong interactions - quantum chromodynamics (QCD), is its nonperturbative behavior in the energy domain typical for nuclear physics. Fortunately, we have a bridge connecting QCD with low-energy phenomena - chiral perturbation theory (ChPT), which enables us to derive effective inter-nucleon interactions. Despite the tremendous progress that has been achieved in the past decade in constructing high-precision realistic 2- and 3-nucleon forces from ChPT [EMN20], [EKR20], *ab-initio* modeling of collective states and, in particular, giant resonances is still limited to light systems. It is still helpful to rely on more phenomenological models, which can provide a better quantitative description of observed data.

The crucial idea in developing a theory of nuclear collective vibrations is to replace fermionic degrees of freedom (nucleons) with boson-like excitations, which serve as building blocks for modeling collective states. This recipe turned out to be very useful in several areas of nuclear physics. Feschbach and Iachello, in their pioneering works [FI74, FI73], used *ph* representation of bosons and showed that spectra of closed-shell nuclei ^{16}O, ^{40}Ca could be described within interacting boson approximation (IBA). From a practical point of view, they replaced many fermionic (single-particle) degrees of freedom with a few collective phonons of bosonic type. The omission of the Pauli principle and an unclear relation to the shell model picture of the nucleus were the main shortcomings of the approach. However, analogously, one can describe low-lying spectra of open-shell nuclei in terms of collective excitations of valence particles. This assumption turned out to be very useful and led to the formulation of the Interacting Boson model (IBM) (Arima and Iachello [AI75], [AI76], [AI78]).

The IBM can be understood as a truncated shell model where identical fermions occupy valence space and form monopole and quadrupole boson-like pairs. This way, one can effectively reduce the number of degrees of freedom and computational cost. The efficacy of IBM led to its spread to many areas of nuclear physics, but approximations adopted in IBM forbade establishing a simple link to more sophisticated microscopic models.

In microscopic approaches, the mean-field picture is the starting approximation that simplifies the solution of the many-body problem. There are two commonly-used ways to determine proper single-particle degrees of freedom. The first one, adopted in most shell model (SM) calculations, extracts single-particle energies from experimental "‘single-particle” levels of neighboring odd nuclei. In the selfconsistent mean-field theories, instead, we employ HF(HFB) method to calculate single-(quasi)particle basis, energies, and residual interactions from the same Hamiltonian. The selfconsistency is crucial for describing nuclear collectivity.

1.2.1 Microscopic models of harmonic vibrations

In the phenomenological models, unknown parameters are tuned to obtain the best agreement of principal characteristics of collective states (energies, transition probabilities) with experimental data. Microscopic models are more ambitious since they attempt to attain a realistic description of collective states from underlying nucleon-nucleon interactions. The microscopic picture is based on the idea of a mean field, which approximates the exact ground state of the nucleus. However, independent particle motion is perturbed by residual nucleon forces, which give rise to the correlations. Indeed, the long-range part of the residual interaction is responsible for the emergence of collective vibrational states. In many cases, such states can be fairly well described by a harmonic approximation. Typical examples are (nearly) harmonic oscillations of the nuclear shape, but also collective vibrations related to other degrees of freedom (e. g., spin-flip transitions, pairing vibrations) were observed in many atomic nuclei.

This section is devoted to the mostly adopted microscopic method used for modeling collective vibrations in nuclei - the Random Phase Approximation (RPA). The derivation of RPA equations, with a detailed discussion about their formal properties, is part of many textbooks (e.g., [RS80],[Row70]); therefore, the discussion is restricted just to crucial aspects of RPA in *ph* formalism.

Let us assume a many-body system described by a 2-body Hamiltonian $\hat{H}$ expressed in second quantization and HF representation

$$\hat{H} = \sum_{ij} \epsilon_i \hat{a}_i^\dagger \hat{a}_i + \sum_{ijkl} V_{ijkl} : \hat{a}_i^\dagger \hat{a}_j^\dagger \hat{a}_l \hat{a}_k : + E_{HF}, \tag{1.9}$$

where $\hat{a}_i^\dagger, \hat{a}_i$ are fermionic creation and annihilation operators and ϵ_i corresponding single-particle energies. We assume that single-particle basis was obtained in a selfconsistent HF calculation and, therefore, the residual 2-body part can be expressed via normal ordering : : with respect to HF vacuum state $|\mathrm{HF}\rangle$ with energy $E_{HF} = \langle \mathrm{HF}| \hat{H} |\mathrm{HF}\rangle$.

The exact ground state $|\tilde{0}\rangle$, excited states $|\lambda\rangle$ and corresponding eigenergies E_0, E_λ can be, in principle, obtained by solving the Schrödinger equation

$$\hat{H} |\lambda\rangle = E_\lambda |\lambda\rangle , \quad \hat{H} |\tilde{0}\rangle = E_0 |\tilde{0}\rangle . \tag{1.10}$$

For strongly interacting many-body systems like nuclei, it is impossible to find exact solutions of equations 1.10, and one has to adopt suitable approximation schemes. Although the strong character of interaction prohibits fast convergence of absolute energies and wave functions, relative observables can still be effectively described without the knowledge of (quasi)exact solutions. In the case of (quasi)harmonic vibrations, one assumes that collective excitations are created by the action of a phonon operator $\hat{Q}_\lambda^\dagger$ on the ground state $|\tilde{0}\rangle$ of the system, i. e.,

$$|\lambda\rangle = \hat{Q}_\lambda^\dagger |\tilde{0}\rangle , \quad \hat{Q}_\lambda |\tilde{0}\rangle = 0. \tag{1.11}$$

The introduction of phonon-like excitations 1.11 allows us to rewrite 1.10 to more convenient form

$$[\hat{H}, \hat{Q}_\lambda^\dagger] |\tilde{0}\rangle = \hbar\omega_\lambda \hat{Q}_\lambda^\dagger |\tilde{0}\rangle , \tag{1.12}$$

where $\hbar\omega_\lambda = E_\lambda - E_0$ denotes the excitation energy. As the phonon operators $\hat{Q}_\lambda^\dagger$ and vacuum state $|\tilde{0}\rangle$ are unknown *a priori*, in practical calculations, some assumptions about their form must be introduced. Their particular choice determines the approximation used in solving the many-body problem[2].

---

[2] In microscopic models, the phonon operator is chosen to capture a general type of excitation, not only a collective one, and allows for treating non-collective (single-particle) and collective states on equal footing.

Following the standard prescription [Row68],[RS80], we evaluate the expectation value of double commutators $[\delta\hat{Q}_{\lambda'},[\hat{H},\hat{Q}^{\dagger}_{\lambda}]]$ in the ground state as

$$\left\langle\tilde{0}\right|[\delta\hat{Q}_{\lambda'},[\hat{H},\hat{Q}^{\dagger}_{\lambda}]]\left|\tilde{0}\right\rangle = \hbar\omega_{\lambda}\left\langle\tilde{0}\right|[\delta\hat{Q}_{\lambda'},\hat{Q}^{\dagger}_{\lambda}]\left|\tilde{0}\right\rangle . \tag{1.13}$$

In the previous expression $\left\langle\tilde{0}\right|\delta\hat{Q}_{\lambda'}$ denotes a general state generated as a variation of phonon operator $\delta\hat{Q}^{\dagger}_{\lambda'}$.

As a starting point, a reasonable approximation of the exact ground state $\left|\tilde{0}\right\rangle$ has to be calculated. In the case of close (sub-)shell nuclei HF (or phenomenological) mean-field state is adopted ($\left|\tilde{0}\right\rangle \approx |\mathrm{HF}\rangle$). In open-shell systems, short-range pairing correlations have to be taken into account. This can be achieved by introducing quasiparticles within HFB theory.

The next step requires construction of a many-body basis suitable for the description of excited states. In the closed-shell systems, elementary *ph* excitations of the HF mean-field and, in the open-shell systems, 2-quasiparticle (*qp)* excitations of the HFB vacuum are used as building blocks of collective excitations. Their mixing, caused by the long-range part of residual interaction, gives rise to the appearance of collective modes. The following discussion is restricted to spherical closed-shell nuclei and *ph* formalism.

The simplest microscopic model of nuclear vibrations, generally known as the Tamm-Dancoff approximation (TDA), assumes that excited states are combinations of elementary *1p-1h* configurations only. Thus, TDA phonon operator of the form is assumed

$$\hat{Q}^{\dagger(TDA)}_{\lambda} = \sum_{ph} X^{\lambda}_{ph}\hat{a}^{\dagger}_{p}\hat{a}_{h}. \tag{1.14}$$

Here the operators $\hat{a}^{\dagger}_{p},\hat{a}_{h}$ create particle, hole states respectively and X^{λ}_{ph} denotes corresponding *ph* amplitude. From the definition 1.14 we see that TDA vacuum is given by HF state because

$$\hat{Q}^{(TDA)}|\mathrm{HF}\rangle = 0. \tag{1.15}$$

Undoubtedly HF vacuum cannot represent an exact ground state of a closed-shell nucleus because correlations caused by the residual interaction can significantly alter independent particle motion. This shortcoming of TDA is partially cured in more sophisticated *ph* theory - Random phase approximation (RPA). In RPA the phonon operator is defined as

$$\hat{Q}^{\dagger(RPA)}_{\lambda} = \sum_{ph} X^{\lambda}_{ph}\hat{a}^{\dagger}_{p}\hat{a}_{h} - Y^{\lambda}_{ph}\hat{a}^{\dagger}_{h}\hat{a}_{p}, \tag{1.16}$$

and the RPA ground state is defined by equation

$$\hat{Q}^{(RPA)}_{\lambda}|\mathrm{RPA}\rangle = 0. \tag{1.17}$$

In practice, RPA state is unknown and therefore further approximation must be adopted to calculate amplitudes $X^{\lambda}_{ph}, Y^{\lambda}_{ph}$. For this purpose we assume a variation of phonon state

$$\delta\hat{Q}^{(RPA)}_{\lambda} = \sum_{ph} \delta X^{\lambda *}_{ph}\hat{a}^{\dagger}_{h}\hat{a}_{p} - \delta Y^{\lambda *}_{ph}\hat{a}^{\dagger}_{p}\hat{a}_{h}, \tag{1.18}$$

and upon insertion into 1.13 we obtain set of equivalent equations

$$\begin{aligned}\langle \mathrm{RPA}|\,[\hat{a}^\dagger_h\hat{a}_p,[\hat{H},\hat{Q}^{\dagger(RPA)}_\lambda]]\,|\mathrm{RPA}\rangle &= \hbar\omega^{(RPA)}_\lambda\,\langle \mathrm{RPA}|\,[\hat{a}^\dagger_h\hat{a}_p,\hat{Q}^{\dagger(RPA)}_\lambda]\,|\mathrm{RPA}\rangle\\ \langle \mathrm{RPA}|\,[\hat{a}^\dagger_p\hat{a}_h,[\hat{H},\hat{Q}^{\dagger(RPA)}_\lambda]]\,|\mathrm{RPA}\rangle &= \hbar\omega^{(RPA)}_\lambda\,\langle \mathrm{RPA}|\,[\hat{a}^\dagger_p\hat{a}_h,\hat{Q}^{\dagger(RPA)}_\lambda]\,|\mathrm{RPA}\rangle\,.\end{aligned}$$

Despite the simple form of phonon operator 1.16, evaluating the aforementioned matrix elements is a complex task if a correlated RPA vacuum state is considered. Therefore, in realistic calculations correlated RPA state is usually replaced by HF vacuum, i. e.,

$$\langle RPA|\,[\hat{a}^\dagger_h\hat{a}_p,\hat{a}^\dagger_{p'}\hat{a}_{h'}]\,|RPA\rangle \approx \langle HF|\,[\hat{a}^\dagger_h\hat{a}_p,\hat{a}^\dagger_{p'}\hat{a}_{h'}]\,|HF\rangle = \delta_{pp'}\delta_{hh'}. \tag{1.19}$$

This widely adopted simplification, generally denoted as the quasiboson approximation (QBA) [BET61], is certainly plausible if the exact ground state does not differ much from HF vacuum. Consistently with 1.19 we can write

$$\langle RPA|\,[\hat{Q}^{(RPA)}_\lambda,\hat{Q}^{\dagger(RPA)}_{\lambda'}]\,|RPA\rangle \approx \delta_{\lambda\lambda'}, \tag{1.20}$$

i. e., the RPA phonons obey bosonic commutation relations within QBA and the Hamiltonian can be expressed in terms of RPA phonon operators as

$$\hat{H} \approx \sum_\lambda \hbar\omega_\lambda \hat{Q}^{\dagger(RPA)}_\lambda \hat{Q}^{(RPA)}_\lambda + E_{RPA}, \tag{1.21}$$

where the energy of the RPA ground state is given by

$$E_{RPA} = E_{HF} - \sum_\lambda \hbar\omega_\lambda \sum_{ph} |Y^\lambda_{ph}|^2. \tag{1.22}$$

From 1.21 it follows that each RPA mode can be interpreted as a harmonic vibration of the ground state with frequency ω_λ. For convenience, RPA equations can be formulated in matrix form

$$\begin{pmatrix}\boldsymbol{A} & \boldsymbol{B}\\ \boldsymbol{B}^* & \boldsymbol{A}^*\end{pmatrix}\begin{pmatrix}\boldsymbol{X}^{\boldsymbol{\lambda}}\\ \boldsymbol{Y}^{\boldsymbol{\lambda}}\end{pmatrix} = \hbar\omega_\lambda\begin{pmatrix}\mathbf{1} & \mathbf{0}\\ \mathbf{0} & \mathbf{-1}\end{pmatrix}\begin{pmatrix}\boldsymbol{X}^{\boldsymbol{\lambda}}\\ \boldsymbol{Y}^{\boldsymbol{\lambda}}\end{pmatrix}, \tag{1.23}$$

where elements of $\boldsymbol{A}$ and $\boldsymbol{B}$ are given by

$$\begin{aligned}A_{php'h'} &= \langle \mathrm{HF}|\,[\hat{a}^\dagger_h\hat{a}_p,[\hat{H},\hat{a}^\dagger_{p'}\hat{a}_{h'}]\,|\mathrm{HF}\rangle\\ B_{php'h'} &= \langle \mathrm{HF}|\,[\hat{a}^\dagger_h\hat{a}_p,[\hat{H},\hat{a}^\dagger_{h'}\hat{a}_{p'}]\,|\mathrm{HF}\rangle\,.\end{aligned}$$

By solving 1.23 we obtain vectors $\boldsymbol{X}^{\boldsymbol{\lambda}}$ and $\boldsymbol{Y}^{\boldsymbol{\lambda}}$ and, thus RPA phonons 1.16 and excitation energies $\hbar\omega_\lambda$. However, absolute values of backward amplitudes $|\boldsymbol{Y}^{\boldsymbol{\lambda}}|$ are expected to be much smaller compared to forward ones $|\boldsymbol{X}^{\boldsymbol{\lambda}}|$; otherwise, QBA 1.19 would not be justified and RPA would break down. The presence of nonzero backward amplitudes $\boldsymbol{Y}^{\boldsymbol{\lambda}}$ implies that vacuum $|\mathrm{RPA}\rangle$ is no longer a mean-field state, but it contains correlated (*2p-2h*) virtual excitations. Therefore RPA is often entitled as *ph* theory with ground state correlations.

By putting $\boldsymbol{Y}^{\boldsymbol{\lambda}} = 0$, RPA equations 1.23 are reverted to TDA. The main benefit of RPA is given by the presence of virtual ground state correlations (i. e. $\boldsymbol{Y}^{\boldsymbol{\lambda}} \neq 0$)

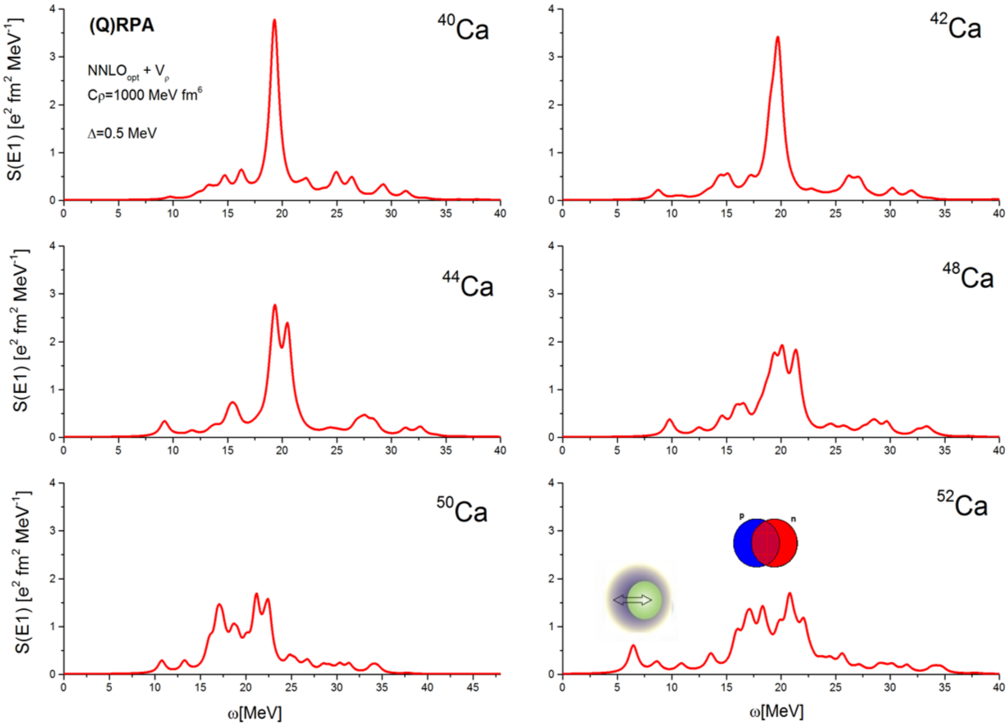

Fig. 1.3: Evolution of isovector dipole strength in Ca isotopes calculated within RPA. With an increasing number of neutrons, the strength is spread over more states and a low-lying bump, interpreted as Pygmy resonance, becomes more prominent. The calculation was carried out with chiral NNLO$_{\mathrm{opt}}$ potential supplemented with a density-dependent phenomenological correction mimicking 3-body contact interaction [KLIV^{+}14]. The strength function was obtained from discrete B(E1) distribution according to prescription 1.2 with $\Delta = 0.5$MeV.

which can significantly enhance transition probabilities of low-lying collective states, in agreement with experimental data.

RPA fulfills several important formal properties. For example, it can be shown that RPA represents a small amplitude limit of time-dependent mean-field methods [RS80]. Moreover, spurious modes connected with symmetry breakings of the mean-field Hamiltonian are separated from physical excitations (see 1.3.3 for more details) in RPA, and RPA strength distributions preserve energy-weighted sum rules. Nowadays, RPA is a routinely used tool for describing low-energy vibrations and GRs of various types in spherical as well as deformed nuclei.

Because of its versatility, RPA was widely adopted in systematic studies of nuclei with purely phenomenological interactions, as well as within the context of modern DFT with effective nuclear forces of nonrelativistic (Skyrme [CCVC13], Gogny [PBB05]) and relativistic type [PRNcvacV03]. Furthermore, in recent years, RPA calculations with realistic 2-body [PPHR06, HPR11, BKI^{+}14], and 2- + 3-body [WHX^{+}18, HWY^{+}20] potentials, were carried out. Since *ab-initio* methods employing modern nucleon potentials are still limited to light, and medium-heavy systems, RPA calculations with realistic forces can serve as an additional testing ground for developing modern nucleon-nucleon potentials suitable for heavier systems.

1.2.2 Extensions of RPA

RPA models, especially the ones based on DFT, were very successful in determining gross characteristics of giant resonances (energy centroids or total transition strengths) across the nuclear chart. However, to describe the widths of GRs and complex low-lying excitations, 1-phonon (or first-order) RPA/TDA methods must be extended. Many-body approaches which extend RPA and incorporate more complex excitations are usually denoted as higher (extended) RPA models. A plethora of such methods was developed and applied in various areas of nuclear physics. A recent comprehensive review of RPA extensions summarized development in this area achieved within the last 20 years [SDD+21].

This section gives a short overview of several state-of-the-art "beyond-RPA" approaches that have been recently successfully implemented in realistic calculations of low-energy collective vibrations and giant resonances.

Second RPA

The most straightforward extension of RPA, second(order) RPA (SRPA) was originally formulated by Sawicky [Saw62], who studied the effect of *2p-2h* states on the spectrum of ^{16}O. Later, a detailed derivation of the SRPA and its relation to general dissipative processes and damping of nuclear collective modes was provided by Yannoules et al. [YDG83, Yan87].

In SRPA, we supplement the phonon operator with terms generating *2p-2h* parts of the wave function. Therefore, the SRPA phonon operator is defined straightforwardly as

$$\begin{aligned}\hat{Q}_{\lambda}^{\dagger(SRPA)} &= \sum_{ph} X_{ph}^{\lambda}\hat{a}_p^{\dagger}\hat{a}_h \quad - \quad Y_{ph}^{\lambda}\hat{a}_p\hat{a}_h^{\dagger} + \\ &+ \sum_{p_1p_2h_1h_2} \mathcal{X}_{p_1p_2h_1h_2}^{\lambda}\hat{a}_{p_1}^{\dagger}\hat{a}_{p_2}^{\dagger}\hat{a}_{h_1}\hat{a}_{h_2} \quad - \quad \mathcal{Y}_{p_1p_2h_1h_2}^{\lambda}\hat{a}_{p_1}\hat{a}_{p_2}\hat{a}_{h_1}^{\dagger}\hat{a}_{h_2}^{\dagger}. \end{aligned} \tag{1.24}$$

In analogy with RPA 1.23, a matrix form of SRPA equations can be derived for amplitudes X^{λ}, Y^{λ} and $\mathcal{X}^{\lambda}, \mathcal{Y}^{\lambda}$ [Yan87, GGC10, PR09]. Without ground state correlations (i. e., backward amplitudes $Y, \mathcal{Y}$ are set to zero) SRPA is reduced to the second(order) TDA (STDA). Unfortunately, the inclusion of *2p-2h* configurations considerably increases the dimensions of model spaces and, therefore, SRPA calculations are computationaly demanding. Thanks to the rapid increase of computational power and the development of numerical libraries in recent years, large-scale SRPA calculations for spherical medium-heavy nuclei became feasible. Including pairing correlations and deformation degrees of freedom leads to an enormous increase in model space dimensions; hence SRPA calculations for deformed nuclei remain beyond the reach of present-day numerical codes.

Large-scale SRPA calculations of electromagnetic responses in selected closed-shell nuclei were carried out with realistic interaction within the framework of the Unitary Correlation Operator Method (UCOM) [PR09, PR10]. SRPA, in general, produces results more consistent with experimental data than RPA (see fig. 1.4). SRPA strength functions are considerably shifted down in energy and more fragmented, which contributes to the spreading width of resonances. On the other hand, some properties of SRPA calculations are problematic. As demonstrated by

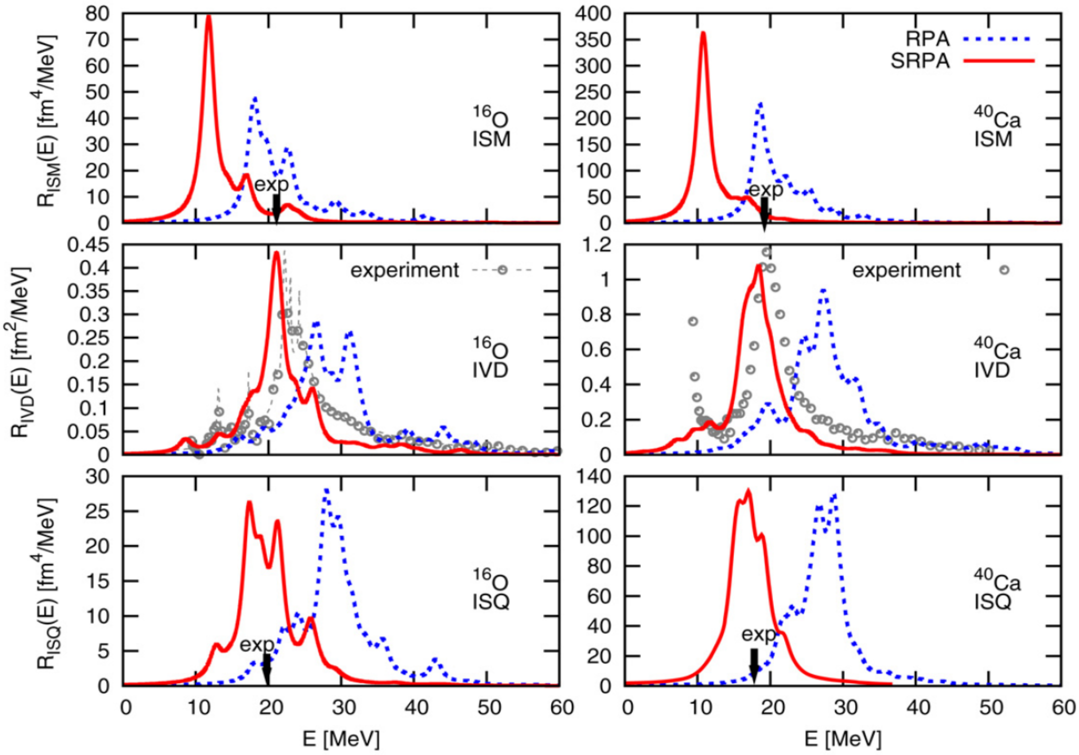

Fig. 1.4: Comparison of RPA and SRPA isoscalar monopole (ISM), isoscalar quadrupole (ISQ) and isovector dipole (IVD) strength functions in ^{16}O and ^{40}Ca. Adopted from [PR09].

Papakonstantinou [Pap14], SRPA might provide unphysical low-lying states and unstable solutions. The problem of instabilities in SRPA and extended RPA was also studied in [Tse13]. Unfortunately, SRPA does not allow the separation of spurious solutions from the physical spectrum, and therefore, low-lying states contain spurious admixtures (see 1.3.3).

Despite the problems mentioned above, SRPA was employed in the context of DFT theories based on Skyrme [GGC10, GGC11, GGE15] and Gogny [GGDD$^+$12] interaction. Recent applications include a systematic study of quadrupole strength up to ^{208}Pb [VGG18] and calculations of dipole strength and polarizability in ^{48}Ca [GGV18]. Moreover, the formalism for charge-exchange transitions was developed and applied to calculations of Gammow-Teller transitions [GGE20] in ^{48}Ca. The influence of tensor force on low-lying $0^+, 2^+, 3^-$states in closed-shell nuclei within SRPA was studied recently [YBSZ21].

SRPA calculations shed light on the nature of quadrupole resonances in spherical closed-shell nuclei. Fine structures of quadrupole strength function in ^{208}Pb [LMv$^+$00], ^{40}Ca[UBC$^+$11] and ^{28}Si [UBC$^+$16] were extracted from high resolution (p, p') and (e, e') experiments and compared with SRPA predictions. These studies confirmed that SRPA accounts for important effects leading to a better description of fragmentation in strength functions and spreading widths of resonances.

Extended theory of Fermi Finite Systems and Quasiparticle Time Blocking Approximation

An alternative many-body approach that uses RPA as an initial step is the Extended theory of Fermi Finite Systems (ETFFS) [KST04]. This self-consistent approach, developed by Migdal [Mig67], is based on the theory of finite Fermi systems and Green-functions formalism. ETFFS naturally extends RPA by including configurations of *1p-1h*×RPA phonon type. In this configuration space, one can derive an effective interaction and charges and consider ground-state correlations in a consistent way. The essential feature of ETFFS is that it incorporates all main sources of resonance widths since it treats continuum effects, Landau damping, as well as complex configurations.

Moreover, ETFFS was combined with covariant relativistic DFT [LRV07, RL09]. Conceptually similar to ETFFS is the Quasiparticle Time Blocking Approximation (QTBA) [LT07], which generalized the Green functions formalism by including *2qp*×RPA phonon configurations. Also, the relativistic version of QTBA (RQTBA) [LRT08] was developed to extend relativistic QRPA. RQTBA was used in several theoretical investigations of low-lying dipole strength distributions, e.g., in the study of dipole excitations in the chain of even-even Calcium isotopes [EL16].

Recently, a finite temperature extension of RQTBA, suitable for studies of highly excited states in medium-heavy nuclei, was presented [WL19]. Further development of the Green functions approach, within the equation of motion framework, made feasible calculations with even more complex *2qp*×2 -phonon states [LS19]. The calculations of dipole response functions in selected Calcium and Nickel isotopes demonstrated that such configurations might induce non-negligible energy shifts and further redistribution of transition strengths.

Particle Vibrational Coupling model

Another example of the method based on RPA, closely related to ETTFS, is Particle Vibrational Coupling (PVC) model [BBB83]. In the PVC, the interaction between low-lying collective states and individual nucleons causes the modification of single-particle states and the damping of giant resonances.

Various PVC calculations can be found in the literature. Whereas older ones rely on phenomenological interactions, modern self-consistent implementations adopt nonrelativistic DFT (with Skyrme interaction) [CSB10], [SCRM20], as well as, relativistic DFT [LR06]. Skyrme effective forces were also employed in extended mean-field theory for a systematic study of coherent and incoherent damping mechanisms of giant resonances in closed-shell nuclei [LAC04].

Quasiparticle-Phonon model

RPA phonons are used as building blocks of the Quasiparticle-Phonon model (QPM), developed by Soloviev and collaborators [Sol92]. In QPM, residual 2-body interaction is approximated by a sum of separable multipole-multipole terms, which allows covering large model spaces with complex states up to 3-phonons in an approximative way. Historically, the separable interaction with adjustable parameters and phenomenological mean-field of Woods-Saxon type were used in the calculations.

The parameters were adjusted in order to describe the properties of low-lying collective transitions.

Once the (Q)RPA phonons $\hat{Q}^{\dagger}_{\lambda}$ are generated, QPM Hamiltonian can be expressed as

$$\hat{H}_{QPM} = \sum_{\lambda} \hbar\omega_{\lambda} \hat{Q}^{\dagger}_{\lambda} \hat{Q}_{\lambda} + \hat{H}_{res}, \tag{1.25}$$

where $\hat{H}_{res}$ describes coupling between multiphonon states (see [Sol92] for details). The Hamiltonian 1.25 is then diagonalized in a truncated multiphonon basis constructed as superpositions of 1-,2-, and 3-phonon states built from low-lying (Q)RPA phonons

$$|\Psi_{\nu}\rangle = \{\sum_{i} X^{\nu}_{i} \hat{Q}^{\dagger}_{i} + \sum_{ij} Y^{\nu}_{ij} \hat{Q}^{\dagger}_{i} \hat{Q}^{\dagger}_{j} + \sum_{ijk} Z^{\nu}_{ijk} \hat{Q}^{\dagger}_{i} \hat{Q}^{\dagger}_{j} \hat{Q}^{\dagger}_{j}\} \, |\Psi_0\rangle \,, \tag{1.26}$$

with ground-state $|\Psi_0\rangle$ calculated in Q(RPA).

The QPM wave functions are properly antisymmetrized since exact commutation relations (beyond QBA) are assumed for (Q)RPA phonons. Moreover, the configuration space spanned by QPM states is large enough for a unified description of low-lying multiphonon states and giant resonances in heavy spherical nuclei [TLS04], as well as systematic studies of low-lying collective states in deformed nuclei (see review [IPS$^+$12]).

Within DFT a self-consistent version of QPM was formulated [TL16] and adopted in the investigation of PDR in Tin isotopic chain [TL08]. QPM has become a powerful theoretical tool for interpretation of data extracted from photon-scattering [SRT$^+$08, OTEL$^+$14], (d,p) and resonant proton scattering [SHB$^+$20], [WSP$^+$21] experiments in medium-heavy and heavy nuclei. Recently, a new high-precision measurement of quadrupole response in ^{112,114}Sn supplemented with QPM calculations has revealed strong evidence of Pygmy quadrupole resonance in these nuclei [TSLZ19].

1.3 Equation of motion phonon method

In the previous section, we gave an overview of selected microscopic methods for describing collective states in nuclei. Coherent superpositions of elementary excitations give rise to the appearance of basic harmonic modes, which can be treated as phonons. It is, therefore, legitimate to use phonons as building blocks of more complex states and express nuclear wave functions as superpositions of multiphonon states in a similar fashion as done in QPM.

The practical obstacle prohibiting calculations in spaces spanned by multiphonon states is a nontrivial evaluation of Hamiltonian in such bases. Straightforward calculation of matrix elements of a general 2-body Hamiltonian is practically unfeasible for more than 2-phonon configurations in J-coupled formalism. On the other hand, the utilization of coupled basis is convenient because it can significantly reduce model space dimensions.

We suggested how to solve this problem in [**AKI$^+$07**], where an iterative method for the exact evaluation of Hamiltonian in bases spanned by TDA multiphonon states was introduced. However, the first application [**AKI$^+$08**] used *1p1h*×TDA phonon configurations and was not fully self-consistent.

The shortcomings were surpassed in the upgraded formulation of the method [**BKLI$^+$12a**] (reprint A.2), which used direct products of TDA phonons, and allowed an effective truncation of multiphonon model spaces. The approach, entitled the Equation of motion phonon method (EMPM), is a natural extension of TDA, accounting for multiphonon configurations. This section summarizes essential steps in the derivation of EMPM and presents several applications in closed-shell and neighboring odd nuclei.

1.3.1 EMPM for even-even systems

The key idea of EMPM is the partitioning of model space into phonon subspaces for which the eigenvalue problem can be solved independently. For this purpose, the full model space $\mathcal{H}$ is decomposed into phonon subspaces $\mathcal{H}_n$

$$\mathcal{H} = \sum_{n=0,1,2...} \oplus \mathcal{H}_n, \tag{1.27}$$

where each subspace is spanned by a set of $n-$phonon states with good angular momenta J. It is convenient to construct such states iteratively as products of TDA phonon operator $\hat{Q}^\dagger_\lambda$ and $(n-1)$-phonon states $|\alpha_{n-1}, J'\rangle \in \mathcal{H}_{n-1}$ according to

$$|(\lambda \times \alpha_{n-1}), JM\rangle = [\hat{Q}^\dagger_\lambda \times |\alpha_{n-1}, J'\rangle]^J_M. \tag{1.28}$$

Here and in the forthcoming text, it is assumed that TDA phonons $\hat{Q}^\dagger_\lambda$ are constructed as spherical tensors of rank J_λ, and the shorthand notation of spherical tensor coupling ($J_\lambda + J' = J$) is used, i. e.,

$$[\hat{Q}^\dagger_\lambda \times |\alpha_{n-1}, J'\rangle]^J_M = \sum_{M_\lambda M'} (J_\lambda M_\lambda J' M' | JM) \hat{Q}^\dagger_{\lambda, J_\lambda M_\lambda} |\alpha_{n-1}, J'M'\rangle \,. \tag{1.29}$$

For simplicity, we also omit angular momenta projections because $J-$coupled formalism allows us to express any quantity in terms of reduced matrix elements.

A general n-phonon state $|\alpha_n, J\rangle \in \mathcal{H}_n$ can be expanded into a basis 1.28

$$|\alpha_n, J\rangle = \sum_{\lambda,\alpha_{n-1}} C^{\alpha_n}_{\lambda\alpha_{n-1}} \, |(\lambda \times \alpha_{n-1}), J\rangle \, . \tag{1.30}$$

The iteration procedure starts for $n = 0$, assuming that the subspace $\mathcal{H}_0$ contains only HF vacuum. Since TDA phonons are built from *1p-1h* excitations , from 1.30 it is obvious that any state $|\alpha_n, J\rangle$ is a linear combination of np-nh configurations only.

Let us search for correlated states 1.30 which diagonalize the Hamiltonian in each $n-$phonon subspace $\mathcal{H}_n$, i. e.,

$$\langle \alpha_n, J| \, \hat{H} \, |\alpha'_n, J'\rangle = E_{\alpha_n} \delta_{\alpha_n,\alpha'_n} \delta_{JJ'}, \qquad n = 0, 1, 2... \tag{1.31}$$

The calculation of eigenenergies E_{α_n} and $n-$phonon eigenstates $|\alpha_n, J\rangle$ requires an evaluation of Hamiltonian matrix in the basis 1.28. However, this task is practically unfeasible in the $J-$coupled scheme for $n > 2$. Instead of direct calculation we assume that states α_{n-1} in the expansion 1.30 diagonalize the Hamiltonian in the subspace $\mathcal{H}_{n-1}$, i. e. eigenvalue problem 1.31 has been already solved for $(n - 1)$. Then, from 1.31 it follows

$$\langle \alpha_n, J| \, [[\hat{H}, \hat{Q}^\dagger_\lambda] \times |\alpha_{n-1}, J'\rangle]^J = (E_{\alpha_n} - E_{\alpha_{n-1}}) \, \langle \alpha_n, J| \, [\hat{Q}^\dagger_\lambda \times |\alpha_{n-1}\rangle]^J. \tag{1.32}$$

The expansion of commutator $[\hat{H}, \hat{Q}^\dagger_\lambda]$ is simple for an uncoupled representation but requires some tedious manipulations in the J scheme. Nevertheless, as we showed in **[BKLI$^+$12a]** (reprint A.2), the equation 1.32 can be rewritten to a generalized eigenvalue problem in $n-$phonon space

$$\mathcal{H}^n C = (\mathcal{A}^n \mathcal{D}^n) C = E^n \mathcal{D}^n C. \tag{1.33}$$

The matrix $\mathcal{H}^n = \mathcal{A}^n \mathcal{D}^n$ is the representation of the Hamiltonian in the basis 1.28

$$(\mathcal{H}^n)_{\lambda\alpha_{n-1},\lambda'\alpha'_{n-1}} = \langle (\lambda \times \alpha_{n-1}), J| \, \hat{H} \, \big|(\lambda' \times \alpha'_{n-1}), J\big\rangle \tag{1.34}$$

and $\mathcal{D}^n$ is the metric (overlap) matrix

$$(\mathcal{D}^n)_{\lambda\alpha_{n-1},\lambda'\alpha'_{n-1}} = \big\langle (\lambda \times \alpha_{n-1}), J \big| (\lambda' \times \alpha'_{n-1}), J \big\rangle \, . \tag{1.35}$$

The expansion coefficients $C^{\alpha_n}_{\lambda\alpha_{n-1}}$ in 1.30 are nothing but components of eigenvectors C in 1.33. In general, the eigenvalue problem 1.33 is defined in overcomplete model space, and one has to extract a linearly independent set of basis states before the diagonalization.

The virtue of EMPM is that matrices $\mathcal{A}^n, \mathcal{D}^n$ in arbitrary n-phonon subspace can be evaluated iteratively from quantities dependent on eigenstates $|\alpha_{n-1}, J\rangle$ of the same Hamiltonian in $(n - 1)$-phonon subspace. In particular, matrix elements of $\mathcal{A}^n, \mathcal{D}^n$ depend on particle-particle (pp) and hole-hole (hh) densities

$$\rho_{\alpha'_{n-1}\alpha_{n-1}}([i \times j]^J) = \langle \alpha_{n-1}, J_{\alpha_{n-1}} || [\hat{a}^\dagger_i \times \hat{b}_j]^J || \alpha'_{n-1}, J_{\alpha'_{n-1}} \rangle, \tag{1.36}$$

and phonon amplitudes

$$X^{\alpha_{n-1}}_{\lambda\alpha_{n-2}} = \langle \alpha_{n-1}, J_{\alpha_{n-1}} || \hat{Q}^\dagger_\lambda || \alpha_{n-2}, J_{\alpha_{n-2}} \rangle. \tag{1.37}$$

The operator $\hat{a}_i^\dagger \equiv \hat{a}_{j_i m_i}^\dagger$, $\hat{b}_i \equiv (-1)^{j_i+m_i}\hat{a}_{j_i -m_i}$ creates particle, hole occupying $i-$th spherical single-particle orbit with angluar momentum j_i and projection m_i, respectively.

Let us notice that densities 1.36 are defined for the states from the same phonon subspace, and therefore pair of indices ij must be either pp or hh type (ph or hp density is zero). The expression for amplitude 1.37, instead, contains states which differ by one phonon. The formulas for iterative calculation of matrix elements 1.34,1.35 can be found in [**BKLI$^+$12a**] (reprint A.2).

Once matrices $\mathcal{A}^n, \mathcal{D}^n$ are calculated we diagonalize $\mathcal{H}^n$ and obtain eigensolutions in $n-$phonon space. The algorithm can be further repeated in $(n+1)$-phonon subspace while keeping its formal simplicity.

After pre-diagonalizations, the Hamiltonian can be formally written as

$$\hat{H} = \sum_n \sum_{\alpha_n, J} E_{\alpha_n} \left|\alpha_n, J\right\rangle \left\langle \alpha_n, J\right| + \sum_{nn', n\neq n'} \sum_{\alpha_n, \alpha'_n, J} \left|\alpha_n, J\right\rangle \hat{H} \left\langle \alpha'_n, J\right| . \tag{1.38}$$

The first term in 1.38 corresponds to diagonal sub-blocks of Hamiltonian in a basis composed of $n-$phonon eigenstates, while the second describes couplings between subspaces with different n. Finally, the total EMPM Hamiltonian matrix, composed of diagonal square blocks and off-diagonal rectangular dense sub-blocks (see fig. 1.5), can be constructed and diagonalized. After the final diagonalisation EMPM eigenstates are given by

$$\left|\Psi, J\right\rangle = \sum_{n=0,1,2...} \sum_{\alpha_n} Z^n_{\alpha_n} \left|\alpha_n, J\right\rangle , \tag{1.39}$$

where $Z^n_{\alpha_n}$ are the amplitudes of multiphonon eigenstates $\{\left|\alpha_n, J\right\rangle, n = 0, 1, 2...\}$.

The EMPM incorporates several approximation schemes, depending on the maximum number of phonons n in the model space. An initial step ($n = 0$) consists in determining a reference state (HF vacuum). EMPM equations are reduced to TDA for $n = 1$. EMPM for $n = 2$ is equivalent to STDA if the ground-state correlations are neglected and all single-particle configurations within a model space are taken into account.

EMPM possesses several advantages compared to STDA and SRPA. Firstly, it can be naturally extended for odd systems and $n > 2$ while preserving the simplicity of formalism. This task is hardly achievable in STDA and SRPA. Since EMPM is formulated solely in the phonon language, calculations requiring a drastic basis truncation are expected to provide more stable results. The second advantage is the treatment of spurious modes connected with the violation of translational invariance of Hamiltonian in many-body calculations. This problem is discussed in section 1.3.3.

Applications of EMPM in closed-shell nuclei

The following part is a short overview of EMPM applications in closed-shell nuclei. Selected papers related to EMPM are enclosed in the appendix of the thesis.

The derivation of EMPM formalism in the angular momentum coupled basis and its first implementation with the inclusion of up to 3-phonon configurations for the description of electric responses in ^{16}O was presented in [**BKLI$^+$12a**] (reprint A.2). Numerical calculations with phenomenological and HF single-particle bases

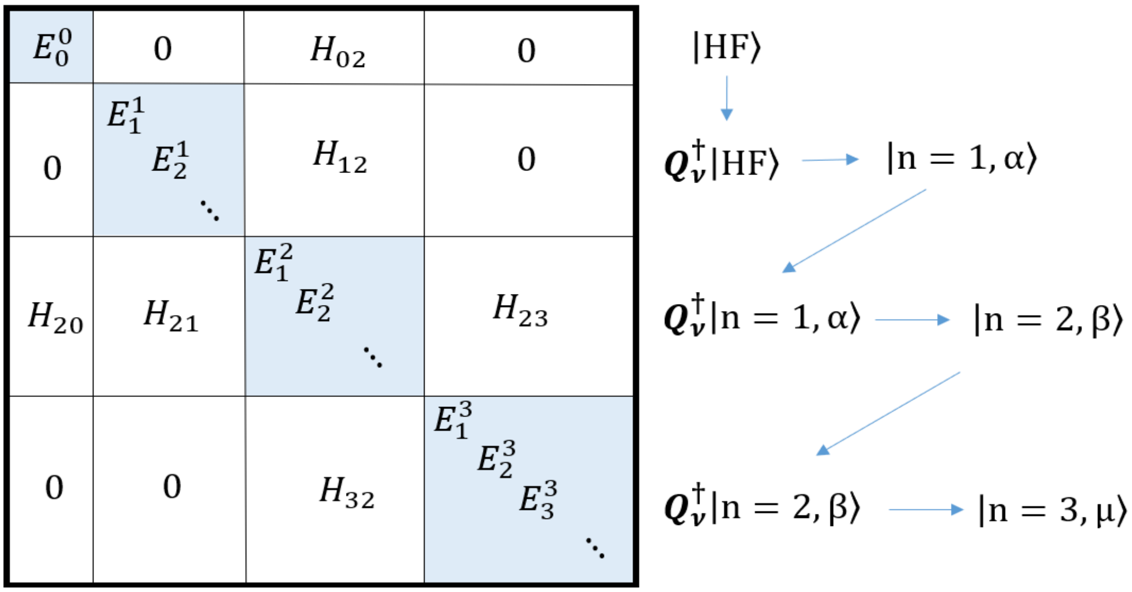

Fig. 1.5: Block-diagonal structure of EMPM matrix for a general 2-body Hamiltonian obtained with the iterative scheme for generating multiphonon states.

demonstrated the effect of 2- and 3-phonon states on strength distributions, as well as ground state correlations. The fragmentation of E1 response in ^{208}Pb was studied in the forthcoming paper [**BKLI$^+$12b**].

The effect of 2-phonon states on ground-state correlation energies of light double magic nuclei was investigated in [**DGHK$^+$17**] (reprint A.5). For this purpose, we adopted Hamiltonian with NNLO$_{opt}$ potential derived from ChPT, which was optimized with the intention of minimizing the effect of 3-body nucleon forces [EBF$^+$13]. We demonstrated that NNLO$_{opt}$ potential provides HF solutions, which account for $\approx$ 40-56 % of total binding energy for light, as well as heavy nuclei (Fig. 1.6).

EMPM calculation showed that missing contribution to ground-state energy of ^{4}He, ^{16}O, ^{40}Ca comes mainly from the coupling between HF and 2-phonon states, but corrections due to the correlations to radii remained tiny and insufficient to describe discrepancies with experimental data. Further, we demonstrated that the 2-phonon components of ground-state wave functions were spread over many states with small individual contributions, but their combined effect produced significant correlation energies. We concluded that the inclusion of coupling between 2- and 4-phonon states would further improve the agreement with the data. However, large dimensions of 4-phonon spaces prohibited such extended EMPM calculations.

NNLO$_{opt}$ potential fails in the description of bulk properties of heavier systems similarly like other soft potentials (UCOM [RPP$^+$06], Daejeon16 [SSK$^+$16], potentials softened by similarity renormalization group approach [RRH08]). It is apparent that a trend of overbinding heavier systems is linked with an underestimation of nuclear radii. From a practical point of view, soft potentials are a preferred choice in many-body calculations because they exhibit a faster convergence of observables in smaller model spaces. A typical undesired feature, however, is an unsatisfactory description of giant resonances in RPA calculations. The energy centroids tend to be systematically shifted to higher energies particularly in heavier nuclei [PPHR06].

Such behavior is typical for all softened nucleon potentials and can be partially cured by introducing a phenomenological density-dependent correction to the in-

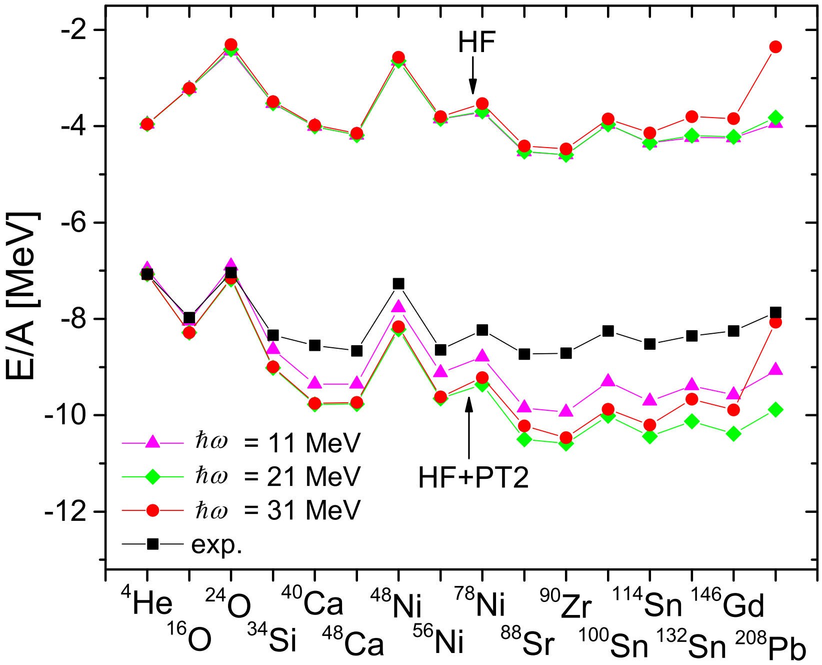

Fig. 1.6: Systematic of ground-state energies calculated from realistic potential NNLO$_{opt}$ within HF approximation and HF + second-order many-body perturbation theory (HF+PT2) . Different colors represent results obtained for several values of $\hbar\omega$ parameter of initial harmonic oscillator single-particle basis. For details see [DGHK^{+}17](reprint A.5).

teraction, which mimics omitted 3-body forces [HPR11, PVK21]. Therefore we adopted such correction in the HF(B)+(Q)RPA and (Q)TDA studies of strength distributions for selected oxygen and tin isotopes **[BKI^{+}14]** (reprint A.1).

EMPM was initially designed as a method for studying fine structures of collective states, especially giant resonances. Calculations up to 2-phonons with NNLO$_{opt}$ potential were carried out to investigate low-lying dipole responses and the spreading widths of IVGDR in ^{132}Sn **[KLIV^{+}14]** (reprint A.3) and ^{208}Pb **[KLIV^{+}15]**. As already pointed out, soft interactions provide single-particle spectra with large energy gaps between major shells resulting in incorrect predictions for GDR energies. Therefore, phenomenological corrections mimicking the effects of 3-body interaction were fitted to reproduce GDR centroids in the abovementioned EMPM calculation. The width and shape of GDR were predicted in EMPM calculations with small smoothening parameter, as the effect of the strong coupling between the 1- and 2-phonon configurations which caused considerable fragmentation of transition strength. Calculated TDA transitions (left panel (a) of 1.7) exhibit several peaks with the most collective part around 13 MeV, whereas EMPM strength function is spread over thousands of states in the same energy region, with significant (or even dominant) 2-phonon components (left panel (b) of 1.7).

The low-lying states around $6 - 8$ MeV remain predominantly 1-phonon, but EMPM predicted many more states. Details, especially in the low-energy part of spectra, depend critically on HF single-particle levels. Therefore EMPM calculations provide an additional information for constructing and fine-tuning of realistic nu-

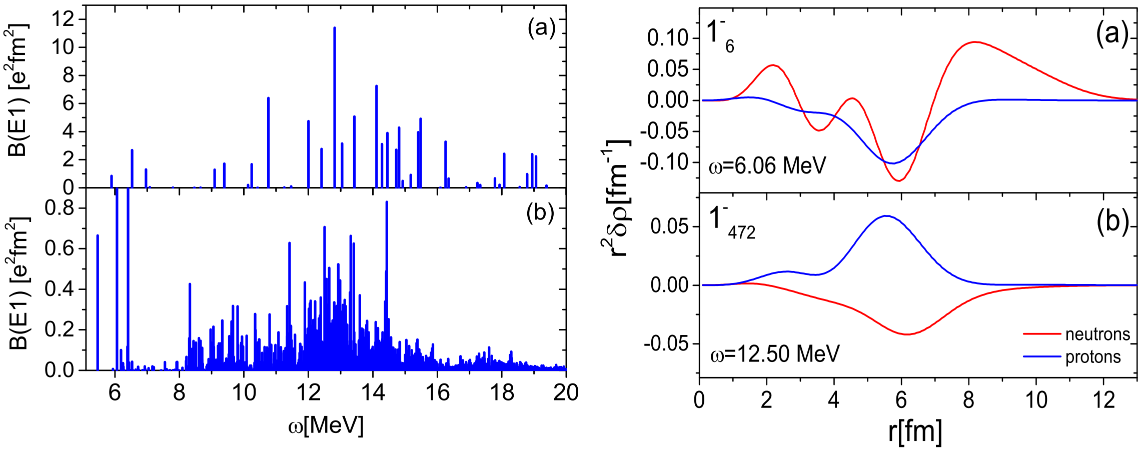

Fig. 1.7: B(E1) strength distributions in ^{208}Pb calculated within TDA (left panel (a)) and EMPM (left panel (b)). Transition densities of selected states corresponding to PDR (right panel (a)) and GDR (right panel (b)) energy regions. Adopted from [KLIV$^+$15].

cleon potentials. Comparison of calculated and experimental photoabsorption cross sections shown in fig. 1.8 demonstrates that EMPM calculation provides better agreement with experimental data than QRPA. Moreover, it is comparable to shell model (SM) calculation with empirical single-particle energies and phenomenological adjustments of effective interaction.

Transition densities calculated within EMPM support a picture of low-lying E1 transitions as oscillations of neutrons against $N = Z$ core (see right panel of 1.7). This picture of PRD resonance is undoubtedly an oversimplification, as demonstrated by Repko et al. [RRNK13], within the Skyrme+RPA model. Their analysis of transition currents revealed that low-energy 1^- states in ^{208}Pb are mixtures of toroidal, compression, and linear flows. EMPM offers an opportunity to investigate how the presence of complicated multiphonon states would alter them. Such investigations are planned for the near future.

Applications of EMPM in open-shell nuclei

So far, the discussion has been reduced to *ph* formalism, limiting thus EMPM to closed-shell systems. In most cases, microscopic models for open-shell nuclei are rooted in the quasiparticle formulation of RPA (TDA) - QRPA(TDA). However, even-even open-shell nuclei exhibit low-energy positive parity valence excitations of different multipolarities, which can be strongly coupled to core excitations of *ph* type. Such states can be effectively described as 2-phonon configurations with unperturbed energies comparable to 1-phonon energies, and therefore the influence of multiphonon configurations on spectra and transitions can be more pronounced than in closed-shell systems.

A generalization of EMPM for open-shell systems is quite straightforward, and the derivation proceeds similarly to the *ph* case discussed before. We start with HFB approximation and calculate the quasiparticle canonical basis. Further, we need to construct QTDA phonons as superpositions of elementary *2qp* excitations. QTDA phonons serve as building blocks for the construction of a multiphonon basis. To evaluate the Hamiltonian matrix in a multiphonon basis, we adopt the same technique, based on commutator equation 1.32, and we derive analogous generalized

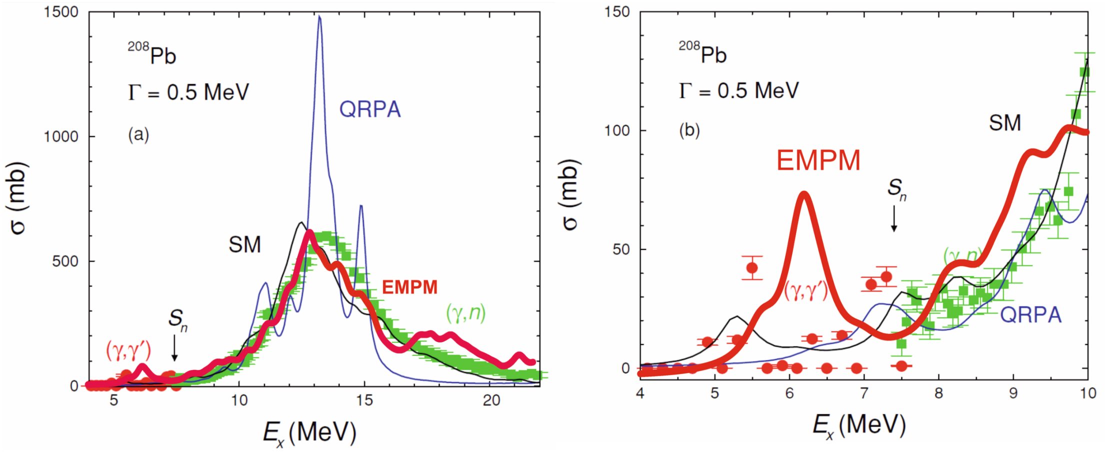

Fig. 1.8: Comparison of photoabsorbtion cross section in ^{208}Pb calculated within QRPA (blue line), SM (black line), and EMPM (red line). Experimental data were extracted from (γ, γ') (red points) and (γ, n) (green points) reactions. The plots were taken and adapted from [SMB+10].

eigenvalue problem 1.33. The derivation of matrix elements of Hamiltonian is rather involved, especially in the $J-$ coupled case. However, final equations possess the same simple structure as in *ph* formulation, though numerical implementation becomes much more involved due to the larger configuration spaces needed in realistic calculations. Quasiparticle EMPM formalism was presented in **[DGKLIV16b]**. As an illustration of its performance and limitations, we investigated spectra and E1 strength in the neutron-rich nucleus ^{20}O. More details can be found in the appendix A.4.

1.3.2 EMPM for systems with valence particle(hole)

This section outlines an extension of EMPM for systems with an odd number of nucleons, precisely, nuclei with one *particle (hole)* outside a close (sub-)shell. The lowest states of such nuclei are expected to have a predominantly single-particle character, which can be considerably disrupted due to the core polarization effects. Since the lowest excitations of spherical nuclei are mainly collective vibrations, coupling between low-lying single-particle states and collective phonons plays a crucial role in the distortion of spectra and response functions.

The idea employed in EMPM for odd nuclei is similar to the even-even case, i. e. an expansion of the wave function describing a state with total angular momentum J to a series of $n-$ phonon states $|\nu_n, J\rangle$ and pre-diagonalization of the Hamiltonian in the subspaces spanned by such states.

In odd-A nucleus $n-$phonon basis can be constructed iteratively by an action of *particle* creation operator $\hat{a}_p^\dagger \equiv a_{j_p m_p}^\dagger$ on a state $|\alpha_n, J'\rangle$ describing an $n-$ phonon excitation of the even-even core, i. e.,

$$|\nu_n, J\rangle = \sum_{p\alpha_n} C_{p\alpha_n}^{\nu_n} |p \times \alpha_n, J\rangle = \sum_{p\alpha_n} C_{p\alpha_n}^{\nu_n} [\hat{a}_p^\dagger \times |\alpha_n, J'\rangle]^J. \tag{1.40}$$

If $|\alpha_n, J'\rangle$ is the eigenstate of Hamiltonian corresponding to the neighboring even-even nucleus in the $n-$ phonon subspace, in virtue of equation 1.31 we can write

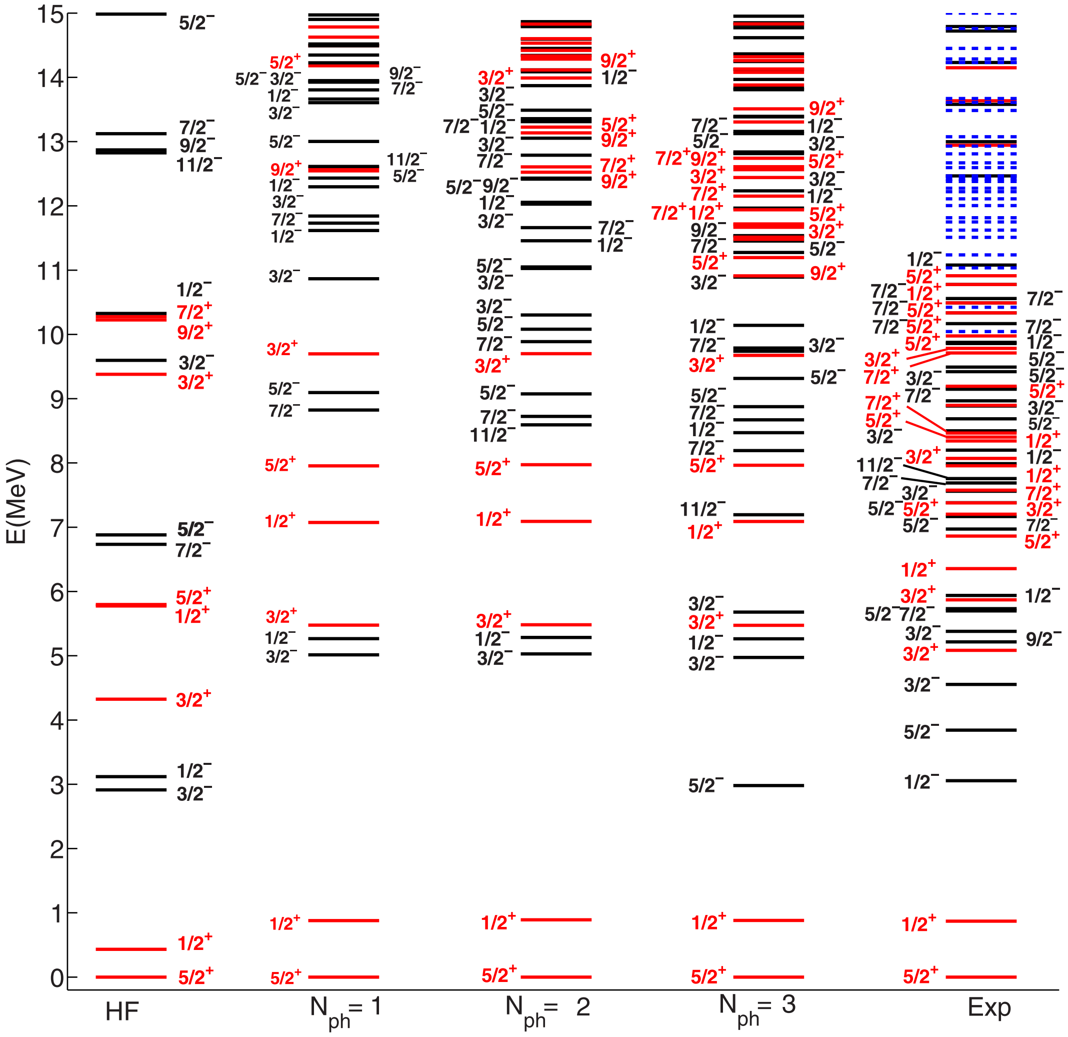

Fig. 1.9: Comparison of experimental and theoretical levels of ^{17}O calculated with EMPM in different multiphonon spaces with maximum phonon number N_{ph}. Dashed lines are levels with unassigned spin and parity. Adapted from **[DGKLIV16a]**.

equation of motion

$$\langle \alpha_n, J| \, [[\hat{a}_p, \hat{H}] \times |\nu_n, J'\rangle]^J = (E_{\nu_n} - E_{\alpha_n}) \, \langle \alpha_n, J| \, [\hat{a}_p \times |\nu_n, J'\rangle]^J, \tag{1.41}$$

where E_{α_n} is the energy of the even-even core. A similar equation can be written for a valence *hole*. In that case, we expand the wave function into

$$|\nu_n, J\rangle = \sum_{p\alpha_n} C^{\nu_n}_{h\alpha_n} \, |h \times \alpha_n, J\rangle = \sum_{h\alpha_n} C^{\nu_n}_{h\alpha_n} [\hat{b}_h \times |\alpha_n, J'\rangle]^J, \tag{1.42}$$

where $\hat{b}_h \equiv (-1)^{j_h + m_h} a_{j_h - m_h}$ creates a hole state in a $j-$ shell, and from 1.31 we get

$$\langle \alpha_n, J| \, [[\hat{b}_h^\dagger, \hat{H}] \times |\nu_n, J'\rangle]^J = (E_{\nu_n} - E_{\alpha_n}) \, \langle \alpha_n, J| \, [\hat{b}_h^\dagger \times |\nu_n, J'\rangle]^J. \tag{1.43}$$

The expansion of the commutators by virtue of the partitioning 1.38 allows us to rewrite equations 1.41 and 1.43 to generalized eigenvalue problem 1.33 with eigenvaules E_{ν_n} describing odd-system with $A+1$ and $A-1$ nucleons, respectively. The Hamiltonian is again given by $\mathcal{A}^n\mathcal{D}^n$, where overlaps of the basis states define

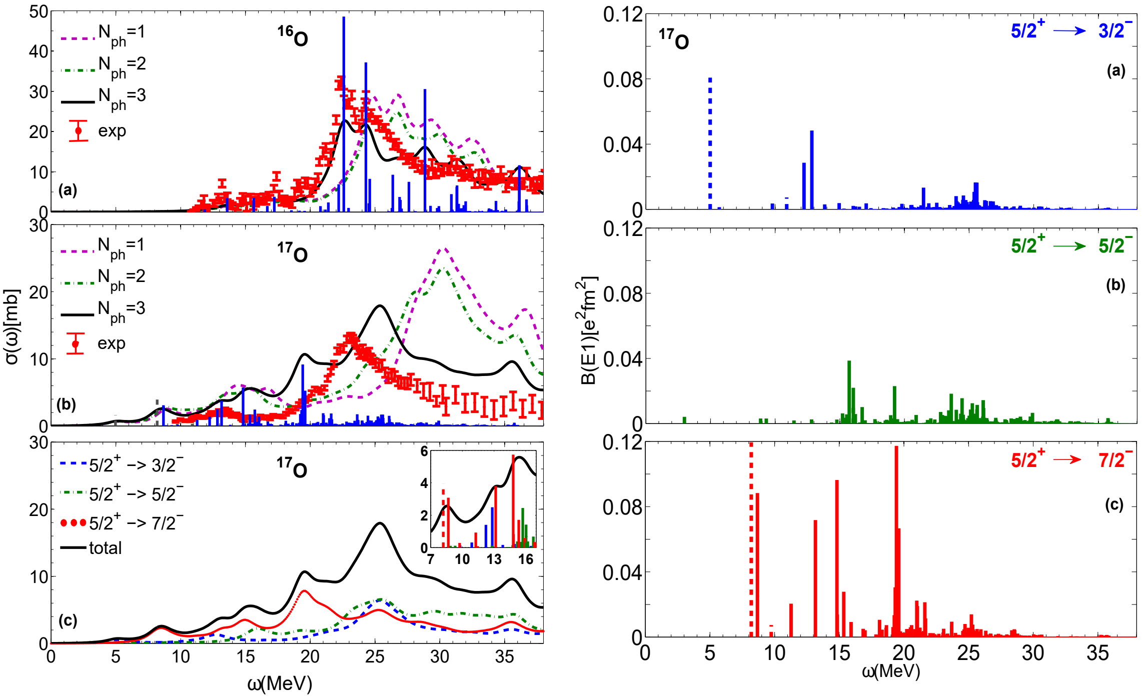

Fig. 1.10: Photoabsorption cross sections in ^{16}O (left panel (a)) and ^{17}O (left panel (b)) calculated in spaces with maximum phonon number N_{ph}. Smoothed contributions from different transitions (left panel (c)) were obtained from discrete E1 strength (right panel) with a Lorentzian of width Δ =2 MeV. The transitions of single-particle nature are plotted as dashed bars. Adopted from **[DKLV17].**

the matrix elements of the metric matrix $\mathcal{D}^n$

$$(\mathcal{D}^n)_{i\alpha_n,i'\alpha'_n} = \langle (i \times \alpha_n), J | (i \times \alpha'_n), J \rangle \,,\ i = p, h. \tag{1.44}$$

It is to be stressed that formal derivation does not impose any approximations and fully respects the Pauli principle and fermionic structure of phonons.

The formulas for calculation of matrices $\mathcal{A}^n$ and $\mathcal{D}^n$ and full Hamiltonian in space spanned by a *particle(hole)*$\times n-$phonon states were, for the first time, presented in **[DGKLIV16a]**. All entering quantities were expressed in terms of $n-$ phonon densities 1.36 and effective potentials between (multi-)phonon and single-particle(hole) states. Such interaction can be easily derived from the original nucleon potential and multiphonon eigenstates of the even-even core.

EMPM for odd systems was firstly employed in calculations of electric quadrupole and magnetic dipole moments and the photoabsorption cross-section in ^{17}O. To be consistent with previous calculations of closed-shell nuclei, we used NNLO$_{opt}$ potential. We found that the inclusion of 1-phonon states improved, in general, the description of low-lying positive parity states, but agreement with experimental levels remained unsatisfactory. The coupling to 2-phonon states did not alter the low-lying spectrum but enhanced the density of states in the region $9-15$ MeV. The inclusion of 3-phonon states would not be feasible without considerable approximations. Due to the enormous number of configurations, the exact calculation of Hamiltonian was too time-consuming. To simplify the calculation, i) we adopted diagonal approximation (i. e., we ignored interaction terms in the matrix elements $\mathcal{A}^n$), ii) we neglected exchange terms in the overlap matrix $\mathcal{D}$, iii) we included only a subset of 2- and 3-phonon states with lowest energies. The overall effect of 1-, 2-

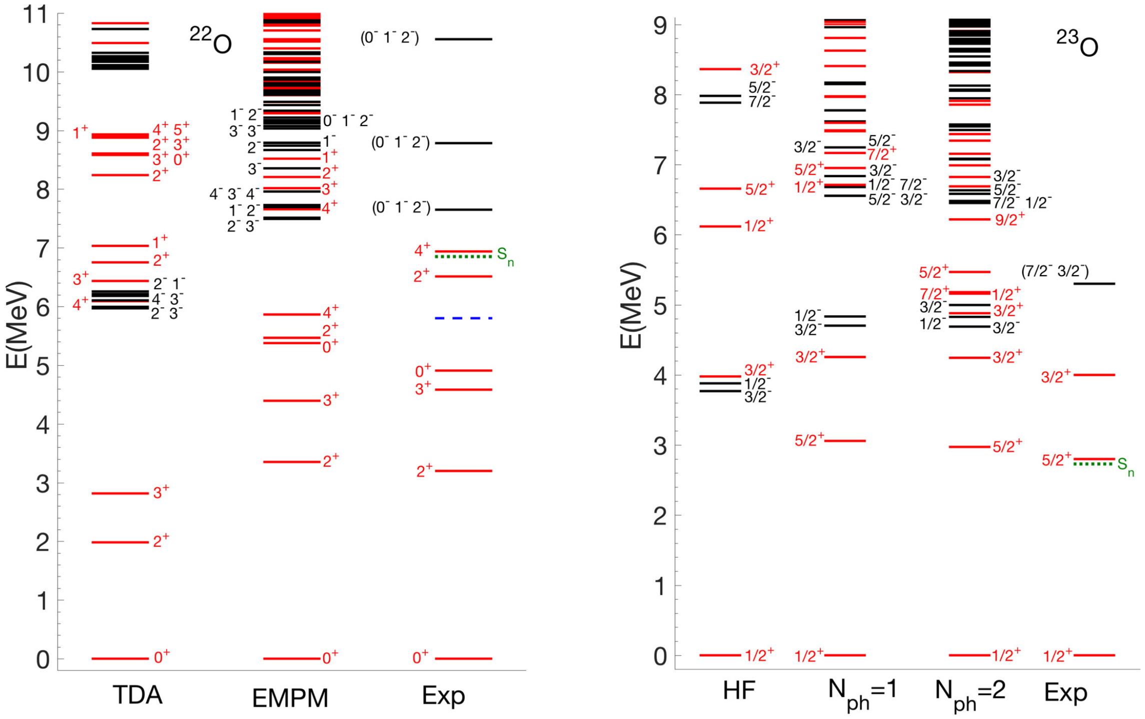

Fig. 1.11: Experimental and theoretical levels of ^{22}O and ^{23}O calculated with EMPM up to 2-phonons. Adopted from [**DKLV18**].

and 3-phonon configurations on the spectrum of ^{17}O is depicted in fig. 1.9. Comprehensive explanation and all formulas can be found in the reprint of the paper A.6.

Further, EMPM was exploited in several theoretical studies of selected medium-heavy odd nuclei. The reprints of two papers are included in Appendix A. In [**DKLV17**] (reprint A.6) we performed a comparative study of spectra, electromagnetic moments, dipole transitions and beta transitions in neutron(proton)-odd nuclei ^{17}O and ^{17}F. Photoabsorption cross-section and electric dipole strength distribution in ^{17}O computed in different approximations are shown on the left panel of fig. 1.10. The inclusion of 3-phonon components significantly pushed dipole strength to lower energies and improved agreement with experimental data, though not enough.

Other papers related to this topic include the study of low-energy levels, dipole strength of ^{23}F, ^{23}O and beta decay of ^{23}F [**DKLV18**] and investigation of nuclei with valence hole in the oxygen region [**DGKLIV19**].

In addition, we extended the formalism to Hamiltonians with 3-body nucleon interactions, treated in the normal-ordered two-body approximation. This modification allowed us to test modern $2+3-$body nucleon interactions such as NNLO$_{sat}$ [EJW$^+$15], within EMPM framework. In principle, such interactions can provide more suitable single-particle spectra and radii without additional phenomenological corrections. In the paper [**DGKLIV20**] (reprint A.7) we investigated odd nuclei around double magic cores ^{16}O and ^{40}Ca with NNLO$_{sat}$ interaction within a refined version of the EMPM which cured a mirror-symmetry violation caused by an incomplete treatment of Pauli principle due to the truncation of phonon basis.

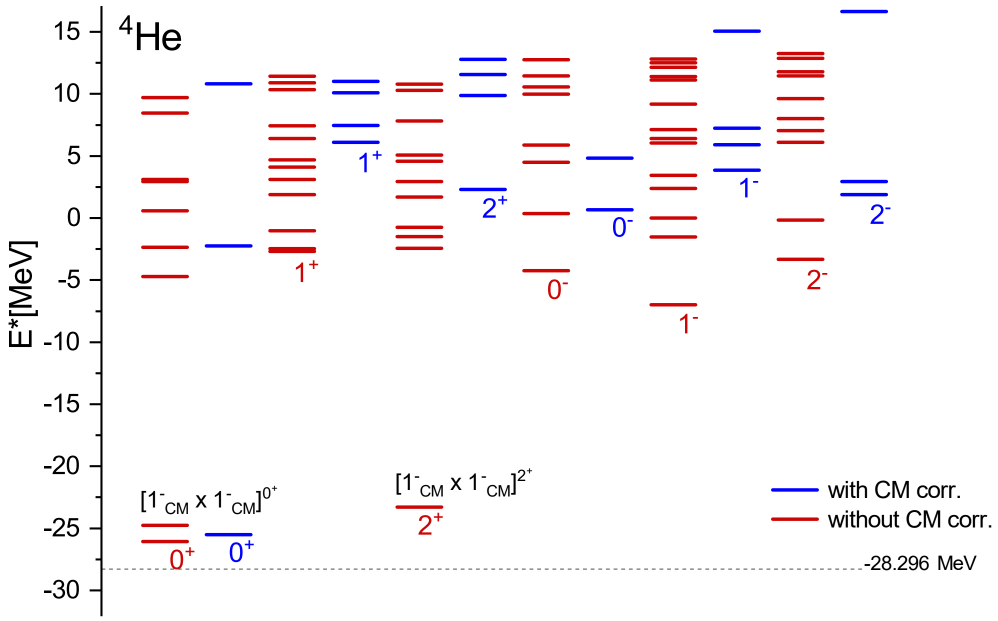

Fig. 1.12: EMPM energy spectrum of ^{4}He calculated up to 3-phonons with (blue) and without CM (red) orthogonalization. The dashed line indicates experimental binding energy.

1.3.3 Center-of-mass problem in EMPM

Nuclear theory practitioners are familiar with the problem of the existence of spurious modes related to the symmetry breaking of Hamiltonian in microscopic calculations. In microscopic models, we introduce a mean-field referred to a fixed origin, which leads to the violation of translational invariance and, consequently, to the appearance of spurious center-of-mass (CM) excitations and their mixing with physical states. Although many methods for obtaining spurious-free states can be found in the literature, complete decoupling of CM motion from physical excitations is in realistic calculations mostly impossible. The exceptions are calculations of few-body systems carried out in Jacobi coordinates and NCSM calculations in complete $N\hbar\omega$ model spaces. This section explains how the CM problem is treated within EMPM.

The indisputable advantage of RPA is the decoupling of spurious states and physical excitations if a self-consistent mean field and corresponding residual interaction are used. In such case, spurious states with zero energy are separated from the rest of the spectrum [Tho61]. However, the finiteness of model spaces in numerical implementations prohibits exact decoupling, and the energy of spurious CM peak approaches zero only if large cutoff energy of unperturbed configurations $(100 - 300$ MeV) is used [CCVC13], [PPHR06]. The CM contamination affects not only excitation energies but influences even more transition probabilities. Typical examples are isoscalar dipole transitions for which a modified transition operator

$$\hat{M}^{IS}_{E1} = \sum_{i=1}^{A} (\hat{r_i}^3 - \frac{5}{3}\langle r^2 \rangle) Y_{1M}(\hat{r}_i) \tag{1.45}$$

have to be used [VS81] in calculations. The second term in 1.45 effectively subtracts spurious CM strength but does not cure wave functions, which remain contaminated, especially if the energy of the CM state significantly differs from zero. Therefore, various methods to eliminate the spuriosity from RPA spectra were suggested [D05],

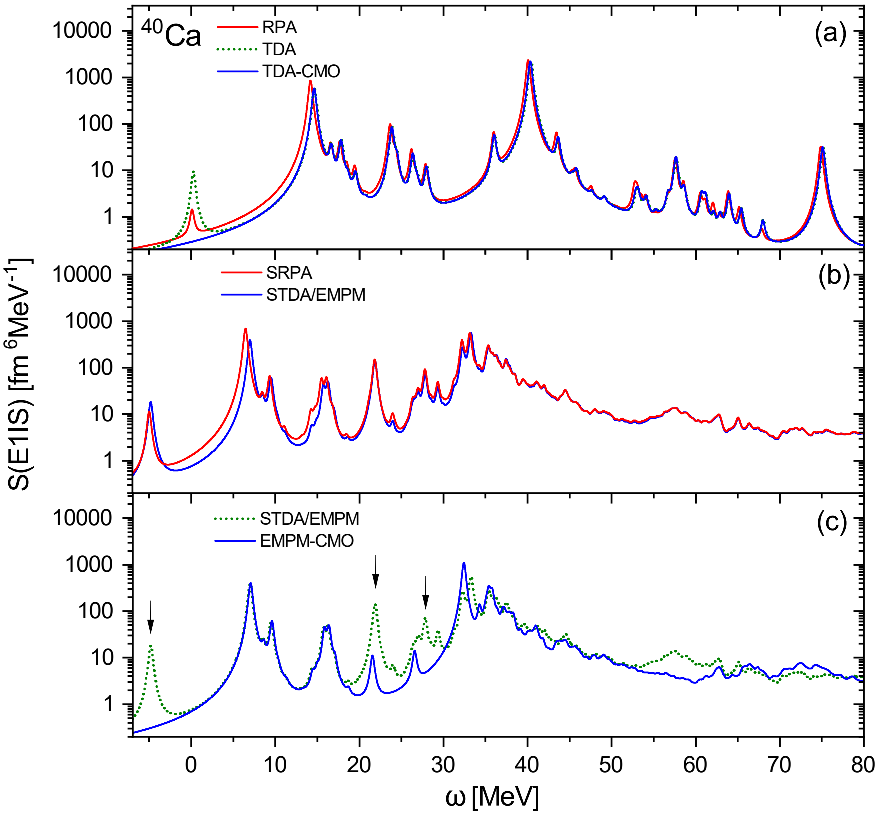

Fig. 1.13: Isoscalar E1 strength functions in ^{40}Ca calculated with different methods by employing UCOM potential. The strengths with (TDA-CMO and EMPM-CMO) and without center-of-mass orthogonalization procedure (TDA, EMPM, STDA, SRPA) are shown for comparison. A single line is drawn for STDA and EMPM since they yield identical results. Arrows indicate states with significant spuriosity.

[RKN19]. Unfortunately, for methods beyond RPA, like extended RPA or SRPA, no simple recipe for the elimination of spurious states exists.

EMPM multiphonon states are constructed from a single-particle basis; therefore, EMPM wave functions would be contaminated by CM motion without special treatment. Our procedure for CM elimination consists of several steps. At the mean-field level, we subtract the CM kinetic energy term and assume the intrinsic Hamiltonian $\hat{H}_{intr} = \hat{H} - \hat{T}_{CM}$. It is to be noted that such correction can be implemented in two ways leading to different single-particle states [JHVB92]. Although HF energy is the same in both cases, second-order perturbative corrections depend on CM treatment. In contrast, EMPM includes complete residual interaction, and EMPM results do not depend on the CM subtraction at the mean-field level.

EMPM basis is built from TDA phonons; therefore, unlike RPA, spurious excitations are mixed with physical states. To avoid this mixing CM state is explicitly constructed from *ph* configurations, and Gramm-Schmidt orthogonalization is used for building a spurious-free TDA basis. Such procedure, described in [**BKI$^+$14**] (reprint A.1), provides clean elimination of CM states from TDA spectra in $J^\pi = 1^-$ channel. The inclusion of multiphonon states makes the CM problem more tricky.

The advantage of using a phonon basis is that we can easily identify all spurious CM components. Multiphonon states 1.28 are created by the action of TDA phonon operator $\hat{Q}^\dagger_\lambda$ on a state belonging to a subspace with the lower number of phonons.

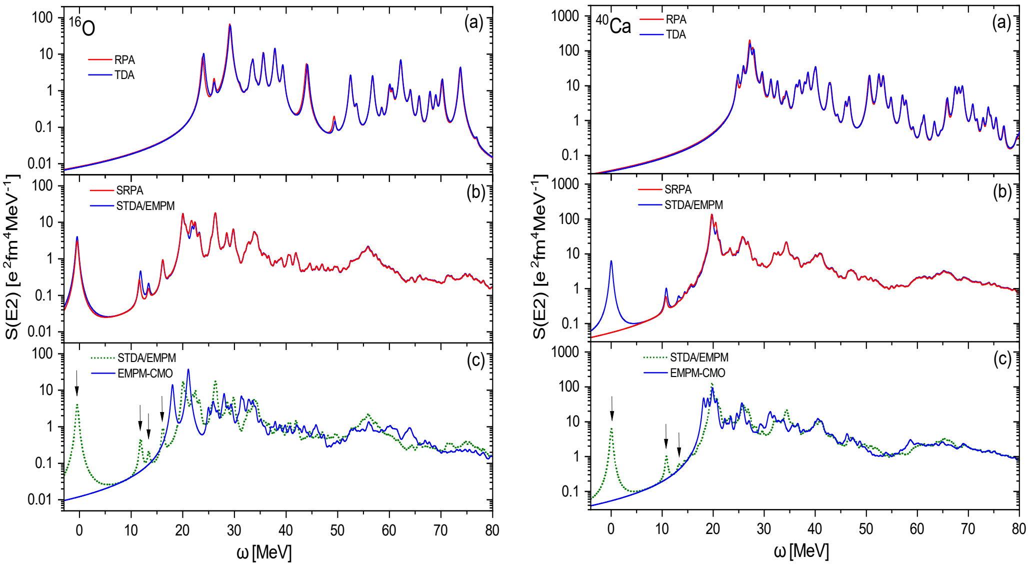

Fig. 1.14: E2 strength functions in ^{16}O and ^{40}Ca calculated with different methods by employing UCOM potential. The strengths with (TDA-CMO and EMPM-CMO) and without center-of-mass orthogonalization procedure (TDA, EMPM, STDA, SRPA) are shown for comparison. A single line is drawn for STDA and EMPM since they yield identical results. Arrows indicate states with significant spuriosity.

Clearly, if we isolate the CM state in TDA, all configurations $[\hat{Q}^{\dagger}_{CM} \times |\alpha_{n-1}, J'\rangle]^{J}$, where $\hat{Q}^{\dagger}_{CM}$ is the spurious CM phonon, are spurious too and have to be discarded from the basis.

Because CM phonon corresponds to $J^{\pi} = 1^{-}$, all 2-phonon states $[\hat{Q}^{\dagger}_{CM} \times |\alpha_{n-1}, J\rangle]^{0^+}, [Q^{\dagger}_{CM} \times |\alpha_{n-1}, J\rangle]^{2^+}, [Q^{\dagger}_{CM} \times |\alpha_{n-1}, J\rangle]^{3^-}$, allowed by angular momentum coupling are spurious, and $0^+, 2^+, 3^-$ spectra become also contaminated. Thus, in numerical calculations, we have to eliminate all states containing spurious phonon $\hat{Q}^{\dagger}_{CM}$ from the basis prior to diagonalization. Such reduction can effectively eliminate the majority of CM contamination in severely truncated model spaces. Nevertheless, due to the nonorthogonality of the multiphonon basis, spurious and physical subspaces remain mutually coupled, and the spectrum can be contaminated even if we reduce the basis by omitting the spurious phonon state. This happens especially in large model spaces where spurious states can be reconstructed due to the overcompletness of multiphonon basis.

To cure this issue, we proposed an effective and easily implementable method based on the singular value decomposition (SVD) of metric submatrix 1.35 between spurious and physical states. We showed that by using SVD, we could transform Hamiltonian to a new basis, decoupled from all spurious excitations. The method was introduced in **[DKLV21]** (reprint A.8), and elaborated in **[DKLV22]** (reprint A.9) in the study of spectroscopic properties of ^{4}He.

The importance of CM decoupling is apparent from fig. 1.12. Without CM orthogonalization, the spectrum is contaminated with many spurious states, which do not correspond to intrinsic excitations. The most insightful are 0^+_2 and 2^+_1 states, which are almost degenerate with the ground state. The analysis of their structure revealed that they are mainly composed of 2-phonon spurious excitations $[\hat{Q}^{\dagger}_{CM} \times$

$\hat{Q}^{\dagger}_{CM}]^{0,2}\,|\mathrm{HF}\rangle$, as expected.

The elimination of CM spuriosity is equally urgent in the calculation of transitions. Figure 1.13 shows isoscalar E1 strength function in ^{40}Ca calculated within EMPM (up to 2-phonons) without CM orthogonalisation procedure, STDA, SRPA and the EMPM with CM removal. Although transition operator 1.45 with CM correction was used, a small transition to the lowest spurious state is seen even in the RPA spectrum. SRPA strength function contains a spurious state with negative energy and, moreover several spurious peaks at energies around 20-30 MeV.

Even pronounced discrepancies can be seen in quadrupole strengths functions (figure 1.14). In the energy below 15 MeV, several spurious peaks are present in STDA, and while some disappear in SRPA (precisely, energies become imaginary), the spectrum remains contaminated in the region of $10 - 15$ MeV. High-energy bumps are similar in all approaches but differ in details.

Compared to other methods, the decisive advantage of EMPM is the use of a phonon basis, which allows for isolating spurious components of model spaces prior to the diagonalization of the Hamiltonian. To our knowledge, there is no solid recipe for eliminating unphysical spuriosities within SRPA.

So far, EMPM calculations of odd nuclei were carried out with CM orthogonalization applied to TDA only, but extending the SVD approach to obtain complete CM motion elimination in odd systems is straightforward. The SVD procedure can be further adapted to exclude spurious states connected with particle number violation in quasiparticle EMPM, which, for open-shell nuclei, is of the same importance as removing CM spuriosity.

The above examples emphasize the need of methods which go beyond RPA that provide reliable results, free of unphysical contaminations. We think that more attention must be devoted to comparing theoretical predictions with experimental data, notable for such phenomena as PDR, whose calculations might be affected by the presence of spurious states.

2. Shell model calculations

The interacting shell model (SM) is one of the cornerstones of nuclear physics, which has been used for decades as a universal tool for understanding the structure of low-lying excitations in nuclei (for a comprehensive review, see [CMPN$^+$05]). In SM, one assumes that low-lying spectra of nuclei can be described with configuration interaction mixing of many-body states, which correspond to particles distributed to only a few orbitals around the Fermi level. This assumption drastically reduces the dimensions of Hamiltonian matrices but requires a calculation of effective interactions adapted to the restricted spaces. Nevertheless, model spaces necessary for calculating spectra in heavy nuclei are still beyond the reach of state-of-the-art SM codes, and therefore, an additional basis reduction is indispensable.

During my post-doctoral stay at Instituto Nazionale di Fisica Nuclear, Sezione di Napoli, I participated in developing the importance sampling (IS) approach for reducing SM model spaces invented by the Naples group. Later, the idea of IS turned out to be very effective in the *ab-initio* no-core shell model (NCSM) calculations. Therefore, in collaboration with the group of T. Dytrych from Institute of Nuclear Physics in Řež, we implemented similar truncation method in the Symmetry-adapted no-core shell model (SA-NCSM).

The following section is a short recap of this work which resulted in the publication of several papers.

2.1 Shell model with important sampling

Model spaces in SM calculations of heavy nuclei easily exceed the limits of present-day numerical codes, which nowadays can solve eigenvalue problems in spaces encompassing up to 10^{10} states. Fortunately, not all basis states are equally important for describing a particular physical observable.

The relative weights of configurations can be examined a posteriori, but it is helpful to estimate their relevance and eliminate them from the model space if possible. Within the SM context, an original diagonalization method of Andreozzi et al. [API02] was invented and later supplemented with IS algorithm [AIP03], which can significantly reduce model space dimensions.

The method was later modified and adapted to a more versatile version employing the uncoupled M-scheme [**BAI$^+$11**] (B.1). The idea of the proposed sampling procedure is to start with a diagonalization of SM Hamiltonian in a subspace of relatively small dimension and, in subsequent iterations, enlarge the space by including new configurations which update the lowest eigenvalues and corresponding eigenvectors. However, not all states from the enlarged model space are kept, just those that lead to considerable changes in eigenvalues. In the optimal case, a convergence of observables for the lowest states is obtained with a small fraction of model space configurations. Thorough description of the algorithm can be found in [**BAI$^+$11**] (reprint B.1) and will not be repeated here. Instead, an overview of the applications of IS method is given below.

The example of SM calculation with IS is shown in fig. 2.1. The calculation of low-energy levels in ^{130,132}Xe was carried out in the valence space spanned by $\{2d_{5/2}, 1g_{7/2}, 2d_{3/2}, 3s_{1/2}, 1h_{11/2}\}$ orbitals, both for protons and neutrons. Protons

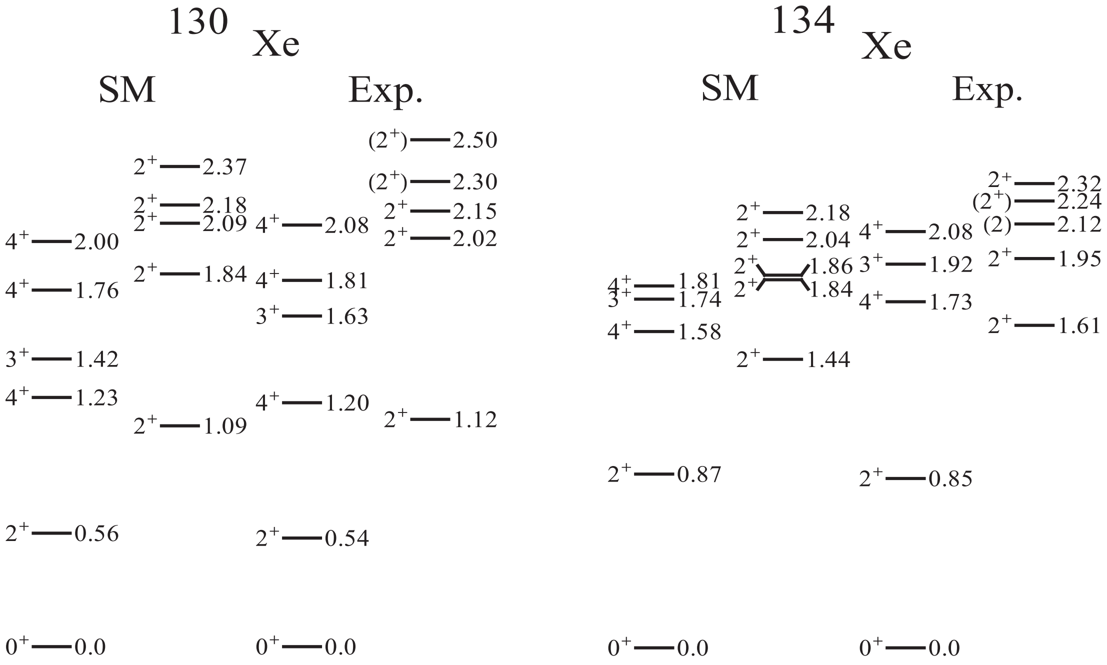

Fig. 2.1: Experimental and theoretical energy spectra of ^{130,134}Xe obtained within SM with IS algorithm. Taken from [**BALI⁺11**].

were included as particles above Z=50 core whereabouts neutrons were treated as holes with respect to N=82 core. Our study showed that $\approx 10\%$ of states was enough for achieving a reasonable convergence of energies in ^{130,132,134}Xe, but the calculation of E2 and M1 transitions in ^{130}Xe required a much larger portion of the model space.

The performance of IS was further tested in the study of low-lying properties of N=80 isotones [**BALI⁺12**] (reprint B.2). The convergence rate and efficiency of sampling were much better than in the case of Xe isotopes. Only a few % of sampled states were necessary to get converged energies. The difference was ascribed to the fact that with an increasing number of neutron holes in Xe isotopes, the deformation of the systems becomes larger. We concluded that a smaller number of configurations is required for nearly spherical shapes; therefore, the sampling is expected to be more effective in regions near magic numbers.

Properties of mixed-symmetry states in Tellurium isotopes were studied in subsequent paper [**BLIA⁺12**] (reprint B.3). The calculation required consideration of more than 20% of the entire model space. Despite severely truncated calculations, we determined collective features of the lowest 2^+ states and their relation to IBM description. Further, systematics of lowest 2^+ states, E2 and M1 transitions in neutron-rich Tellurium and Xenon isotopes were investigated in [**BLIA⁺13**] (see fig. 2.2).

2.2 Importance truncation in SA-NCSM

An alternative to IS was suggested by Roth [RN07, Rot09] within NCSM. Here the sampling criterion is inspired by many-body perturbation theory. The idea is to define a reference state $|\Psi_{ref}\rangle$ which is an eigenstate of effective Hamiltonian $\hat{H}_0$ in reasonably small (reference) model space, i. e. $\hat{H}_0\,|\Psi_{ref}\rangle = \epsilon_{ref}\,|\Psi_{ref}\rangle$. For a

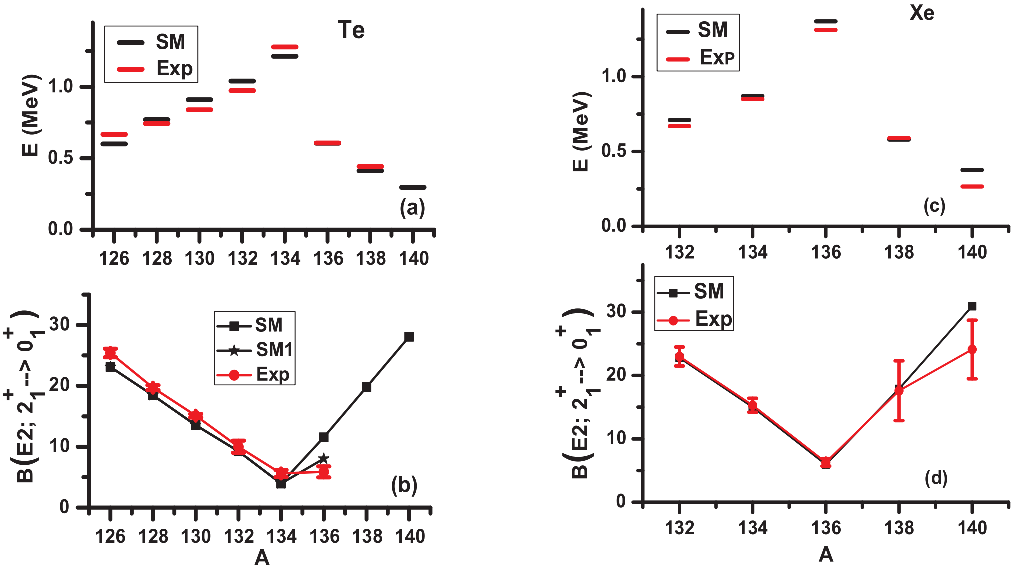

Fig. 2.2: Systematics of 2_1^+ states and B(E2,$2_1^+ \to 0_0^+$) in Xe and Te isotopes calculated within SM with IS algorithm. Transition probabilities are given in Weisskopf units. Taken from [**BLIA**$^+$**13**].

basis state $|\Phi_\nu\rangle$ outside the reference model space, one can evaluate an importance measure parameter according to equation

$$\kappa_\nu = -\frac{\langle\Phi_\nu|\,\hat{H}\,|\Psi_{ref}\rangle}{\epsilon_\nu - \epsilon_{ref}}, \tag{2.1}$$

where $\epsilon_\nu = \langle\Phi_\nu|\,\hat{H}\,|\Phi_\nu\rangle$. The state $|\Phi_\nu\rangle$ is included into enlarged model space if $|\kappa_\nu| > \kappa_{min} > 0$, where κ_{min} is an numerical threshold controlling an acceptance limit, and thus the dimension of the model space. Clearly, all states are included in the model space for $\kappa_{min} \to 0$. The size of κ_ν is correlated with the size of amplitude $C_\nu = |\,\langle\psi|\Phi_\nu\rangle\,|$, where the state $|\psi\rangle$ is an eigenstate of the Hamiltonian obtained in the full model space.

The evaluation of parameter 2.1 prior the diagonalisation can be used to sample only relevant states and, thus, drastically reduce model space dimensions while keeping a reasonable precision of calculated wave functions. This technique, denoted as the Importance-Truncated NCSM (IT-NCSM), was widely employed in NCSM calculations of heavier nuclei which would be prohibited in the complete model spaces. Moreover, a typical monotonic convergence of eigenvalues in IT-NCSM is suitable for using extrapolation techniques and estimating errors introduced by the truncation. [KJN$^+$13].

We implemented an analogous sampling procedure in SA-NCMS. SA-NCSM is an *ab-initio* many-body configuration approach that uses SU(3) coupling scheme for generating basis states and calculation of Hamiltonian matrix elements [LDD16]. Unlike the standard NCSM, SA-NCSM employs physically relevant many-body states with a specific structure (large deformation, minimal total intrinsic spin of protons and neutrons) to reduce model spaces. The selection of basis states is based on physical arguments and qualified guesses which configurations are expected to contribute to nuclear properties under study.

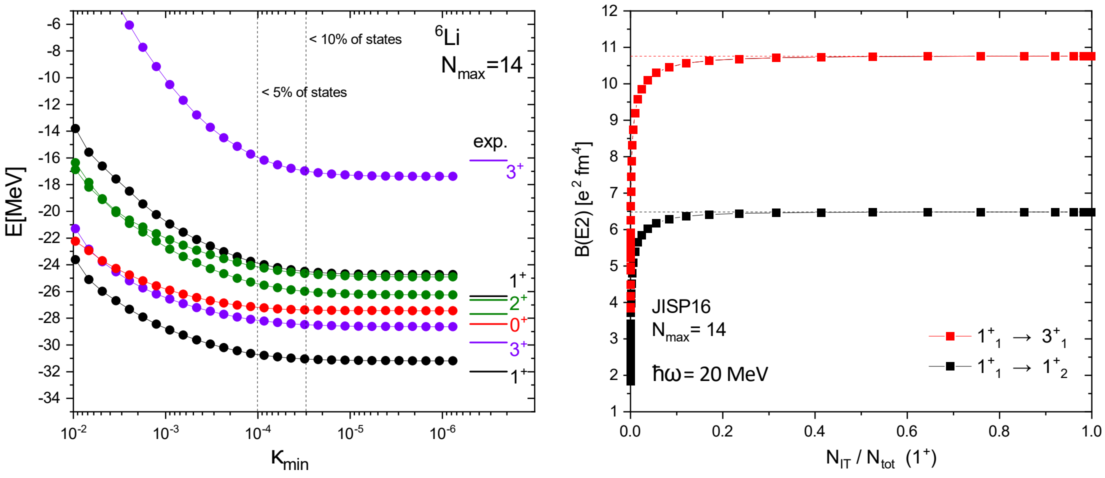

Fig. 2.3: Convergence of spectrum (left) and transitions (right) in ^{6}Li obtained in SA-NCSM with the importance truncation of basis. Horizontal lines indicate values of importance measure parameter threshold κ_{min} corresponding to 5% and 10% of basis states (= $N_{IT}/N_{tot} \times 100$, where N_{IT} denotes number of sampled states and N_{tot} is total number of states. JISP16 nucleon potential was employed in the calculation.

The importance measure parameter 2.1, instead, offers a precise numerical criterion for the selection of basis states. The efficacy of the importance truncation in SA-NCSM was illustrated on "proof of principle" calculation of energy spectrum of ^{6}Li [**KDLO18**], and later, on the calculation of ground-state rotational band in ^{12}C [**KDLO19**] (reprint B.4). We showed that only a fraction of total model space ($\approx$ 3%) was needed to get $\approx$ 96% of binding energy, and an even smaller portion of basis vectors ($\approx$ 9%) was sufficient for the description of excitation energies of lowest states. It is noteworthy that this approach performs similar reductions of the basis as the sampling method discussed in the previous subsection, regardless of the different definitions of sampling criteria.

For illustration, a typical convergence plot in SA-NCSM calculation with importance truncation is shown on the left panel of fig. 2.3, where the evolution of the low-lying spectrum of ^{6}Li with decreasing threshold κ_{min} is depicted. The accuracy of wave functions is essential in the calculations of transition probabilities. Right panel of 2.3 shows fast convergence of quadrupole transitions from the ground state to lowest 1^+_2 and 3^+_1 excited states.

The potential of importance truncation in SA-NCSM calculations has not been fully exploited so far, but we believe that the method can significantly extend the applicability of SA-NCSM to much heavier nuclei. An effective implementation, however, requires an involved on-fly calculation of Hamiltonian matrix elements in SU(3) basis on large high-performance computing systems, a task that will hopefully be accomplished in the future.

Conclusion

This thesis summarized my work devoted to the theoretical modeling of atomic nuclei. I was primarily focused on developing microscopic many-body methods for the description of low-energy collective vibrations and giant resonances. With my collaborators, we developed a new computational scheme designed to treat anharmonic effects and multiphonon excitations in spherical nuclei near magic numbers. In our investigations of nuclear spectra and electromagnetic responses, we employed realistic nucleon potentials and provided complementary insight into several unsolved problems related to the construction of nucleon forces.

Another class of models discussed in the thesis is the shell model and symmetry-adapted no-core shell. This part of our work was devoted to investigations of truncation schemes that would push the limits of shell model calculations to heavier systems. We demonstrated that such truncation algorithms effectively reduce model spaces, but nontrivial technical issues in the implementation of massively parallelized computer codes must be solved in the future to exhaust their potential.

Several directions for further investigations are offered. In the near future, we plan EMPM calculations of energy spectra and giant resonances in odd-nuclei in the lead region, with an emphasis on low-lying dipole strength below the neutron separation energy. Optimization and parallelization of present computer codes and investigation of various truncation strategies which grasp physically relevant states will be necessary for that purpose.

Our preliminary studies show that a promising strategy how to extend EMPM calculations is the employment of alternative single-particle bases, e. g. natural orbitals, recently introduced in several approaches [FCC$^+$22, HTH$^+$21]. As a first step, we plan to benchmark EMPM formulated in natural orbitals basis in light systems with our previous calculations.

Further, we plan to develope a selfconsistent multiphonon scheme for systems with two valence nucleons that would allow us to study the interplay between pair-like and core excitations in semi-magic nuclei.

For completeness, I attach the list of papers that I co-authored and are related to topics discussed in the thesis.

- Equation of motion phonon method

Physical Review C 85, 014313 (2012)
Physical Review C 86, 044327 (2012)
Journal of Physics G: Nuclear and Particle Physics 41, 025109 (2014)
Physical Review C 90, 014310 (2014)
Physical Review C 92, 054315 (2015)
Physical Review C 93, 044314 (2016)
Physical Review C 94, 061301(R) (2016)
Physical Review C 95, 024306 (2017)
Physical Review C 95, 034327 (2017)
Physical Review C 97, 034311 (2018)
Physical Review C 99, 014316 (2019)

Physical Review C 101, 024308 (2020)
Physics Letters B 821 136636 (2021)
Physical Review C 105, 024326 (2022)

- Shell model

Journal of Physics G: Nuclear and Particle Physics 38, 025103 (2011)
Physical Review C 84, 024310 (2011)
Physical Review C 85, 034332 (2012)
Physical Review C 86, 044325 (2012)
Physical Review C 88, 024303 (2013)
Acta Physica Polonica B 50, 541 (2019)

Complete list of publications can be found in ORCID:
https://orcid.org/0000-0002-7708-6290.

Bibliography

[AI75] A. Arima and F. Iachello. Collective nuclear states as representations of a su(6) group. *Phys. Rev. Lett.*, 35:1069–1072, 1975.

[AI76] A Arima and F Iachello. Interacting boson model of collective states i. the vibrational limit. *Annals of Physics*, 99(2):253–317, 1976.

[AI78] A Arima and F Iachello. Interacting boson model of collective nuclear states ii. the rotational limit. *Annals of Physics*, 111(1):201–238, 1978.

[AIP03] F Andreozzi, N Lo Iudice, and A Porrino. An importance sampling algorithm for generating exact eigenstates of the nuclear hamiltonian. *Journal of Physics G: Nuclear and Particle Physics*, 29(10):2319–2333, sep 2003.

[AKI$^+$07] F. Andreozzi, F. Knapp, N. Lo Iudice, A. Porrino, and J. Kvasil. Exact formulation and solution of the nuclear eigenvalue problem in a microscopic multiphonon space. *Phys. Rev. C*, 75:044312, 2007.

[AKI$^+$08] F. Andreozzi, F. Knapp, N. Lo Iudice, A. Porrino, and J. Kvasil. Multiphonon nuclear response in ^{16}O: A microscopic treatment equivalent to the shell model. *Phys. Rev. C*, 78:054308, Nov 2008.

[API02] F Andreozzi, A Porrino, and N Lo Iudice. A simple iterative algorithm for generating selected eigenspaces of large matrices. *Journal of Physics A: Mathematical and General*, 35(5):L61–L66, jan 2002.

[BAI$^+$11] D Bianco, F Andreozzi, N Lo Iudice, A Porrino, and F Knapp. A diagonalization algorithm revisited and applied to the nuclear shell model. *Journal of Physics G: Nuclear and Particle Physics*, 38(2):025103, jan 2011.

[BALI$^+$11] D. Bianco, F. Andreozzi, N. Lo Iudice, A. Porrino, and F. Knapp. Matrix diagonalization algorithm and its applicability to the nuclear shell model. *Phys. Rev. C*, 84:024310, Aug 2011.

[BALI$^+$12] D. Bianco, F. Andreozzi, N. Lo Iudice, A. Porrino, and F. Knapp. Importance-sampling diagonalization algorithm for large-scale shell model calculations on $\mathbf{N = 80}$ isotones. *Phys. Rev. C*, 85:034332, Mar 2012.

[BBB83] G. F. Bertsch, P. F. Bortignon, and R. A. Broglia. Damping of nuclear excitations. *Rev. Mod. Phys.*, 55:287–314, Jan 1983.

[BET61] G.E. Brown, J.A. Evans, and D.J. Thouless. Vibrations of spherical nuclei. *Nuclear Physics*, 24(1):1–17, 1961.

[BF75] B. L. Berman and S. C. Fultz. Measurements of the giant dipole resonance with monoenergetic photons. *Rev. Mod. Phys.*, 47:713–761, Jul 1975.

[BKI+14] D Bianco, F Knapp, N Lo Iudice, P Veselý, F Andreozzi, G De Gregorio, and A Porrino. A self-consistent study of multipole response in neutron-rich nuclei using a modified realistic potential. *Journal of Physics G: Nuclear and Particle Physics*, 41(2):025109, 2014.

[BKLI+12a] D. Bianco, F. Knapp, N. Lo Iudice, F. Andreozzi, and A. Porrino. Upgraded formulation of the nuclear eigenvalue problem in a microscopic multiphonon basis. *Phys. Rev. C*, 85:014313, 2012.

[BKLI+12b] D. Bianco, F. Knapp, N. Lo Iudice, F. Andreozzi, A. Porrino, and P. Vesely. Electric dipole response in ^{208}pb within a new microscopic multiphonon approach. *Phys. Rev. C*, 86:044327, Oct 2012.

[BLIA+12] D. Bianco, N. Lo Iudice, F. Andreozzi, A. Porrino, and F. Knapp. Mixed-symmetry states in te isotopes within a large-scale shell model approach. *Phys. Rev. C*, 86:044325, Oct 2012.

[BLIA+13] D. Bianco, N. Lo Iudice, F. Andreozzi, A. Porrino, and F. Knapp. Spectroscopy of neutron-rich te and xe isotopes within a new shell model context. *Phys. Rev. C*, 88:024303, Aug 2013.

[BLT19] A. Bracco, E.G. Lanza, and A. Tamii. Isoscalar and isovector dipole excitations: Nuclear properties from low-lying states and from the isovector giant dipole resonance. *Progress in Particle and Nuclear Physics*, 106:360–433, 2019.

[CCVC13] Gianluca Colò, Ligang Cao, Nguyen Van Giai, and Luigi Capelli. Self-consistent rpa calculations with skyrme-type interactions:the skyrme rpa program. *Computer Physics Communications*, 184(1):142–161, 2013.

[CDF+22] J. Carter, L.M. Donaldson, H. Fujita, Y. Fujita, M. Jingo, C.O. Kureba, M.B. Latif, E. Litvinova, F. Nemulodi, P. von Neumann-Cosel, R. Neveling, P. Papakonstantinou, P. Papka, L. Pellegri, V.Yu. Ponomarev, A. Richter, R. Roth, E. Sideras-Haddad, F.D. Smit, J.A. Swartz, A. Tamii, R. Trippel, I.T. Usman, and H. Wibowo. Damping of the isovector giant dipole resonance in 40,48ca. *Physics Letters B*, page 137374, 2022.

[CMPN+05] E. Caurier, G. Martínez-Pinedo, F. Nowacki, A. Poves, and A. P. Zuker. The shell model as a unified view of nuclear structure. *Rev. Mod. Phys.*, 77:427–488, 2005.

[CSB10] Gianluca Colò, Hiroyuki Sagawa, and Pier Francesco Bortignon. Effect of particle-vibration coupling on single-particle states: A consistent study within the skyrme framework. *Phys. Rev. C*, 82:064307, Dec 2010.

[D0̈5] F. Dönau. Suppression of modes in the random phase approximation. *Phys. Rev. Lett.*, 94:092503, 2005.

[DGHK$^+$17] G. De Gregorio, J. Herko, F. Knapp, N. Lo Iudice, and P. Veselý. Ground-state correlations within a nonperturbative approach. *Phys. Rev. C*, 95:024306, 2017.

[DGKLIV16a] G. De Gregorio, F. Knapp, N. Lo Iudice, and P. Vesely. Microscopic multiphonon method for odd nuclei and its application to ^{17}O. *Phys. Rev. C*, 94:061301, 2016.

[DGKLIV16b] G. De Gregorio, F. Knapp, N. Lo Iudice, and P. Vesely. Self-consistent quasiparticle formulation of a multiphonon method and its application to the neutron-rich ^{20}O nucleus. *Phys. Rev. C*, 93:044314, 2016.

[DGKLIV19] G. De Gregorio, F. Knapp, N. Lo Iudice, and P. Veselý. Microscopic multiphonon approach to nuclei with a valence hole in the oxygen region. *Phys. Rev. C*, 99:014316, 2019.

[DGKLIV20] G. De Gregorio, F. Knapp, N. Lo Iudice, and P. Veselý. Proper treatment of the pauli principle in mirror nuclei within the microscopic particle(hole)-phonon scheme. *Phys. Rev. C*, 101:024308, 2020.

[DKLV17] G. De Gregorio, F. Knapp, N. Lo Iudice, and P. Veselý. Low- and high-energy spectroscopy of ^{17}O and ^{17}F within a microscopic multiphonon approach. *Phys. Rev. C*, 95:034327, 2017.

[DKLV18] G. De Gregorio, F. Knapp, N. Lo Iudice, and P. Veselý. Microscopic multiphonon approach to spectroscopy in the neutron-rich oxygen region. *Phys. Rev. C*, 97:034311, Mar 2018.

[DKLV21] G. De Gregorio, F. Knapp, N. Lo Iudice, and P. Veselý. Removal of the center of mass in nuclei and its effects on 4he. *Physics Letters B*, 821:136636, 2021.

[DKLV22] G. De Gregorio, F. Knapp, N. Lo Iudice, and P. Veselý. Spectroscopic properties of ^{4}He within a multiphonon approach. *Phys. Rev. C*, 105:024326, 2022.

[EBF$^+$13] A. Ekström, G. Baardsen, C. Forssén, G. Hagen, M. Hjorth-Jensen, G. R. Jansen, R. Machleidt, W. Nazarewicz, T. Papenbrock, J. Sarich, and S. M. Wild. Optimized chiral nucleon-nucleon interaction at next-to-next-to-leading order. *Phys. Rev. Lett.*, 110:192502, 2013.

[EJW$^+$15] A. Ekström, G. R. Jansen, K. A. Wendt, G. Hagen, T. Papenbrock, B. D. Carlsson, C. Forssén, M. Hjorth-Jensen, P. Navrátil, and W. Nazarewicz. Accurate nuclear radii and binding energies from a chiral interaction. *Phys. Rev. C*, 91:051301, 2015.

[EKR20] E. Epelbaum, H. Krebs, and P. Reinert. High-precision nuclear forces from chiral eft: State-of-the-art, challenges, and outlook. *Frontiers in Physics*, 8, 2020.

[EL16] Irina A. Egorova and Elena Litvinova. Electric dipole response of neutron-rich calcium isotopes in relativistic quasiparticle time blocking approximation. *Phys. Rev. C*, 94:034322, Sep 2016.

[EMN20] D. R. Entem, R. Machleidt, and Y. Nosyk. Nucleon-nucleon scattering up to n5lo in chiral effective field theory. *Frontiers in Physics*, 8, 2020.

[FCC+22] Patrick J. Fasano, Chrysovalantis Constantinou, Mark A. Caprio, Pieter Maris, and James P. Vary. Natural orbitals for the ab initio no-core configuration interaction approach. *Phys. Rev. C*, 105:054301, May 2022.

[FI73] H. Feshbach and F. Iachello. The interacting boson model structure of ^{16}O. *Physics Letters B*, 45(1):7–11, 1973.

[FI74] H. Feshbach and F. Iachello. The interacting boson model. *Annals of Physics*, 84(1):211–231, 1974.

[GGC10] D. Gambacurta, M. Grasso, and F. Catara. Collective nuclear excitations with skyrme-second random-phase approximation. *Phys. Rev. C*, 81:054312, May 2010.

[GGC11] D. Gambacurta, M. Grasso, and F. Catara. Low-lying dipole response in the stable ^{40,48}ca nuclei with the second random-phase approximation. *Phys. Rev. C*, 84:034301, Sep 2011.

[GGDD+12] D. Gambacurta, M. Grasso, V. De Donno, G. Co', and F. Catara. Second random-phase approximation with the gogny force: First applications. *Phys. Rev. C*, 86:021304, 2012.

[GGE15] D. Gambacurta, M. Grasso, and J. Engel. Subtraction method in the second random-phase approximation: First applications with a skyrme energy functional. *Phys. Rev. C*, 92:034303, Sep 2015.

[GGE20] D. Gambacurta, M. Grasso, and J. Engel. Gamow-teller strength in ^{48}Ca and ^{78}Ni with the charge-exchange subtracted second random-phase approximation. *Phys. Rev. Lett.*, 125:212501, 2020.

[GGV18] D. Gambacurta, M. Grasso, and O. Vasseur. Electric dipole strength and dipole polarizability in 48ca within a fully self-consistent second random–phase approximation. *Physics Letters B*, 777:163–168, 2018.

[Gor98] S. Goriely. Radiative neutron captures by neutron-rich nuclei and the r-process nucleosynthesis. *Physics Letters B*, 436(1):10–18, 1998.

[GT48] M. Goldhaber and E. Teller. On nuclear dipole vibrations. *Phys. Rev.*, 74:1046–1049, Nov 1948.

[HPR11] H. Hergert, P. Papakonstantinou, and R. Roth. Quasiparticle random-phase approximation with interactions from the similarity renormalization group. *Phys. Rev. C*, 83:064317, 2011.

[HTH⁺21] J. Hoppe, A. Tichai, M. Heinz, K. Hebeler, and A. Schwenk. Natural orbitals for many-body expansion methods. *Phys. Rev. C*, 103:014321, Jan 2021.

[HvdW01] M.N. Harakeh and A. van der Woude. *Giant Resonances*. Oxford Science Publications, 2001.

[HWY⁺20] B. S. Hu, Q. Wu, Q. Yuan, Y. Z. Ma, X. Q. Yan, and F. R. Xu. Nuclear multipole responses from chiral effective field theory interactions. *Phys. Rev. C*, 101:044309, 2020.

[IPS⁺12] N Lo Iudice, V Yu Ponomarev, Ch Stoyanov, A V Sushkov, and V V Voronov. Low-energy nuclear spectroscopy in a microscopic multiphonon approach. *Journal of Physics G: Nuclear and Particle Physics*, 39(4):043101, mar 2012.

[JHVB92] L. Jaqua, M. A. Hasan, J. P. Vary, and B. R. Barrett. Kinetic-energy operator in the effective shell-model interaction. *Phys. Rev. C*, 46:2333–2339, 1992.

[KDLO18] F. Knapp, T. Dytrych, D. Langr, and T. Oberhuber. Importance truncation in the su(3) symmetry-adapted no-core shell model. *Acta Physica Polonica B Proceedings Supplement*, 11:65–72, 2018.

[KDLO19] F. Knapp, T. Dytrych, D. Langr, and T. Oberhuber. Importance basis truncation in the symmetry-adapted no-core shell model. *Acta Physica Polonica B*, 50:541–547, 2019.

[KJN⁺13] M. K. G. Kruse, E. D. Jurgenson, P. Navrátil, B. R. Barrett, and W. E. Ormand. Extrapolation uncertainties in the importance-truncated no-core shell model. *Phys. Rev. C*, 87:044301, Apr 2013.

[KLIV⁺14] F. Knapp, N. Lo Iudice, P. Veselý, F. Andreozzi, G. De Gregorio, and A. Porrino. Dipole response in ^{132}Sn within a self-consistent multiphonon approach. *Phys. Rev. C*, 90:014310, 2014.

[KLIV⁺15] F. Knapp, N. Lo Iudice, P. Veselý, F. Andreozzi, G. De Gregorio, and A. Porrino. Dipole response in ^{208}Pb within a self-consistent multiphonon approach. *Phys. Rev. C*, 92:054315, 2015.

[KST04] S. Kamerdzhiev, J. Speth, and G. Tertychny. Extended theory of finite fermi systems: collective vibrations in closed shell nuclei. *Physics Reports*, 393(1):1–86, 2004.

[Kva22] J. Kvasil. Nuclear structure and nuclear processes. https://ipnp.cz/~kvasil/lectures/nuclear%20structure%20and%20nuclear%20processes/NS+NR.pdf, 2022.

[LAC04] D. Lacroix, S. Ayik, and Ph. Chomaz. Nuclear collective vibrations in extended mean-field theory. *Progress in Particle and Nuclear Physics*, 52(2):497–563, 2004.

[LDD16] Kristina D. Launey, Tomas Dytrych, and Jerry P. Draayer. Symmetry-guided large-scale shell-model theory. *Progress in Particle and Nuclear Physics*, 89:101–136, 2016.

[LMv$^+$00] D. Lacroix, A. Mai, P. von Neumann-Cosel, A. Richter, and J. Wambach. Multiple scales in the fine structure of the isoscalar giant quadrupole resonance in 208pb. *Physics Letters B*, 479(1):15–20, 2000.

[LR06] E. Litvinova and P. Ring. Covariant theory of particle-vibrational coupling and its effect on the single-particle spectrum. *Phys. Rev. C*, 73:044328, Apr 2006.

[LRT08] E. Litvinova, P. Ring, and V. Tselyaev. Relativistic quasiparticle time blocking approximation: Dipole response of open-shell nuclei. *Phys. Rev. C*, 78:014312, Jul 2008.

[LRV07] E. Litvinova, P. Ring, and D. Vretenar. Relativistic rpa plus phonon-coupling analysis of pygmy dipole resonances. *Physics Letters B*, 647(2):111–117, 2007.

[LS19] Elena Litvinova and Peter Schuck. Toward an accurate strongly coupled many-body theory within the equation-of-motion framework. *Phys. Rev. C*, 100:064320, Dec 2019.

[LT07] E. V. Litvinova and V. I. Tselyaev. Quasiparticle time blocking approximation in coordinate space as a model for the damping of the giant dipole resonance. *Phys. Rev. C*, 75:054318, May 2007.

[Mig67] A. B. Migdal. *Theory of Finite Fermi Systems and Application to Atomic Nuclei.* Wiley, New York, 1967.

[NCvT19] P. Neumann-Cosel von and A. Tamii. Electric and magnetic dipole modes in high-resolution inelastic proton scattering at 0°. *European Physical Journal A*, 55, 2019.

[NuP15] NuPECC. Nupecc brochure "light to reveal the heart of matter". 2015.

[OTEL$^+$14] B. Özel-Tashenov, J. Enders, H. Lenske, A. M. Krumbholz, E. Litvinova, P. von Neumann-Cosel, I. Poltoratska, A. Richter, G. Rusev, D. Savran, and N. Tsoneva. Low-energy dipole strength in ^{112,120}Sn. *Phys. Rev. C*, 90:024304, Aug 2014.

[Pap14] P. Papakonstantinou. Second random-phase approximation, thouless' theorem, and the stability condition reexamined and clarified. *Phys. Rev. C*, 90:024305, Aug 2014.

[PBB05] S. Peru, J. S. Berger, and P. F. Bortignon. Giant resonances in exotic spherical nuclei within the rpa approach with the gogny force. *The European Physical Journal A - Hadrons and Nuclei*, 26:25–32, 2005.

[PFK$^+$14] I. Poltoratska, R. W. Fearick, A. M. Krumbholz, E. Litvinova, H. Matsubara, P. von Neumann-Cosel, V. Yu. Ponomarev, A. Richter, and A. Tamii. Fine structure of the isovector giant dipole resonance in ^{208}Pb: Characteristic scales and level densities. *Phys. Rev. C*, 89:054322, May 2014.

[PPHR06] N. Paar, P. Papakonstantinou, H. Hergert, and R. Roth. Collective multipole excitations based on correlated realistic nucleon-nucleon interactions. *Phys. Rev. C*, 74:014318, 2006.

[PR09] P. Papakonstantinou and R. Roth. Second random phase approximation and renormalized realistic interactions. *Physics Letters B*, 671(3):356–360, 2009.

[PR10] P. Papakonstantinou and R. Roth. Large-scale second random-phase approximation calculations with finite-range interactions. *Phys. Rev. C*, 81:024317, 2010.

[PRNcvacV03] N. Paar, P. Ring, T. Nikšić, and D. Vretenar. Quasiparticle random phase approximation based on the relativistic hartree-bogoliubov model. *Phys. Rev. C*, 67:034312, Mar 2003.

[PVK21] P. Papakonstantinou, J. P. Vary, and Y. Kim. Daejeon16 interaction with contact-term corrections for heavy nuclear systems. *Journal of Physics G: Nuclear and Particle Physics*, 48(8):085105, 2021.

[RKN19] A. Repko, J. Kvasil, and V. O. Nesterenko. Elimination of spurious modes within quasiparticle random-phase approximation. *Phys. Rev. C*, 99:044307, 2019.

[RL09] P Ring and E. V. Litvinova. Particle-vibrational coupling in covariant density-functional theory. *Physics of Atomic Nuclei*, 72:1285–1304, 2009.

[RN07] R. Roth and P. Navrátil. Ab initio study of ^{40}Ca with an importance-truncated no-core shell model. *Phys. Rev. Lett.*, 99:092501, Aug 2007.

[Rot09] Robert Roth. Importance truncation for large-scale configuration interaction approaches. *Phys. Rev. C*, 79:064324, Jun 2009.

[Row68] D. J. Rowe. Equations-of-motion method and the extended shell model. *Rev. Mod. Phys.*, 40:153–166, 1968.

[Row70] D. J. Rowe. *Nuclear collective motion*. Springer US, 1970.

[RPP$^+$06] R. Roth, P. Papakonstantinou, N. Paar, H. Hergert, T. Neff, and H. Feldmeier. Hartree-fock and many body perturbation theory with correlated realistic nn interactions. *Phys. Rev. C*, 73:044312, 2006.

[RRH08] R. Roth, S. Reinhardt, and H. Hergert. Unitary correlation operator method and similarity renormalization group: Connections and differences. *Phys. Rev. C*, 77:064003, 2008.

[RRNK13] A. Repko, P.-G. Reinhard, V. O. Nesterenko, and J. Kvasil. Toroidal nature of the low-energy $e1$ mode. *Phys. Rev. C*, 87:024305, 2013.

[RS80] P. Ring and P. Schuck. *The Nuclear Many-Body Problem.* Springer-Verlag New York, 1980.

[Saw62] J. Sawicki. Higher random phase approximation and energy spectra of spherical nuclei. *Phys. Rev.*, 126:2231–2238, 1962.

[SCRM20] Shihang Shen, Gianluca Colò, and Xavier Roca-Maza. Particle-vibration coupling for giant resonances beyond the diagonal approximation. *Phys. Rev. C*, 101:044316, Apr 2020.

[SD50] Helmut Steinwedel and J.Hans D.Jensen. Hydrodynamik von kerndipolschwingungen. *Zeitschrift für Naturforschung A*, 5(8):413–420, 1950.

[SDD+21] P. Schuck, D.S. Delion, J. Dukelsky, M. Jemai, E. Litvinova, G. Röpke, and M. Tohyama. Equation of motion method for strongly correlated fermi systems and extended rpa approaches. *Physics Reports*, 929:1–84, 2021. Equation of Motion Method for strongly correlated Fermi systems and Extended RPA approaches.

[SHB+20] M. Spieker, A. Heusler, B. A. Brown, T. Faestermann, R. Hertenberger, G. Potel, M. Scheck, N. Tsoneva, M. Weinert, H.-F. Wirth, and A. Zilges. Accessing the single-particle structure of the pygmy dipole resonance in ^{208}Pb. *Phys. Rev. Lett.*, 125:102503, 2020.

[SMB+10] R. Schwengner, R. Massarczyk, B. A. Brown, R. Beyer, F. Dönau, M. Erhard, E. Grosse, A. R. Junghans, K. Kosev, C. Nair, G. Rusev, K. D. Schilling, and A. Wagner. $e1$ strength in ^{208}Pb within the shell model. *Phys. Rev. C*, 81:054315, May 2010.

[Sol92] V.G. Soloviev. *Theory of Atomic Nuclei, Quasi-particle and Phonons.* Taylor & Francis, 1992.

[SRT+08] R. Schwengner, G. Rusev, N. Tsoneva, N. Benouaret, R. Beyer, M. Erhard, E. Grosse, A. R. Junghans, J. Klug, K. Kosev, H. Lenske, C. Nair, K. D. Schilling, and A. Wagner. Pygmy dipole strength in ^{90}Zr. *Phys. Rev. C*, 78:064314, Dec 2008.

[SSK+16] A.M. Shirokov, I.J. Shin, Y. Kim, M. Sosonkina, P. Maris, and J.P. Vary. N3lo nn interaction adjusted to light nuclei in ab exitu approach. *Physics Letters B*, 761:87–91, 2016.

[SY93] S. Shlomo and D. H. Youngblood. Nuclear matter compressibility from isoscalar giant monopole resonance. *Phys. Rev. C*, 47:529–536, Feb 1993.

[Tho61] D.J. Thouless. Vibrational states of nuclei in the random phase approximation. *Nuclear Physics*, 22(1):78–95, 1961.

[TL08] N. Tsoneva and H. Lenske. Pygmy dipole resonances in the tin region. *Phys. Rev. C*, 77:024321, Feb 2008.

[TL16] N. Tsoneva and H. Lenske. Energy–density functional plus quasiparticle–phonon model theory as a powerful tool for nuclear structure and astrophysics. *Physics of Atomic Nuclei*, 79:885–903, 2016.

[TLS04] N Tsoneva, H Lenske, and Ch Stoyanov. Probing the nuclear neutron skin by low-energy dipole modes. *Physics Letters B*, 586(3):213–218, 2004.

[Tse13] V. I. Tselyaev. Subtraction method and stability condition in extended random-phase approximation theories. *Phys. Rev. C*, 88:054301, Nov 2013.

[TSLZ19] N. Tsoneva, M. Spieker, H. Lenske, and A. Zilges. Fine structure of the pygmy quadrupole resonance in 112,114sn. *Nuclear Physics A*, 990:183–198, 2019.

[UBC$^+$11] I. Usman, Z. Buthelezi, J. Carter, G.R.J. Cooper, R.W. Fearick, S.V. Förtsch, H. Fujita, Y. Fujita, Y. Kalmykov, P. von Neumann-Cosel, R. Neveling, P. Papakonstantinou, A. Richter, R. Roth, A. Shevchenko, E. Sideras-Haddad, and F.D. Smit. Fine structure of the isoscalar giant quadrupole resonance in 40ca due to landau damping? *Physics Letters B*, 698(3):191–195, 2011.

[UBC$^+$16] I. T. Usman, Z. Buthelezi, J. Carter, G. R. J. Cooper, R. W. Fearick, S. V. Förtsch, H. Fujita, Y. Fujita, P. von Neumann-Cosel, R. Neveling, P. Papakonstantinou, I. Pysmenetska, A. Richter, R. Roth, E. Sideras-Haddad, and F. D. Smit. Fine structure of the isoscalar giant quadrupole resonance in ^{28}Si and ^{27}Al. *Phys. Rev. C*, 94:024308, Aug 2016.

[VGG18] O. Vasseur, D. Gambacurta, and M. Grasso. Systematic study of giant quadrupole resonances with the subtracted second random-phase approximation: Beyond-mean-field centroids and fragmentation. *Phys. Rev. C*, 98:044313, Oct 2018.

[VS81] Nguyen Van Giai and H. Sagawa. Monopole and dipole compression modes in nuclei. *Nuclear Physics A*, 371(1):1–18, 1981.

[WHX$^+$18] Q. Wu, B. S. Hu, F. R. Xu, Y. Z. Ma, S. J. Dai, Z. H. Sun, and G. R. Jansen. Chiral nnlo$_{\mathrm{sat}}$ descriptions of nuclear multipole resonances within the random-phase approximation. *Phys. Rev. C*, 97:054306, 2018.

[WL19] Herlik Wibowo and Elena Litvinova. Nuclear dipole response in the finite-temperature relativistic time-blocking approximation. *Phys. Rev. C*, 100:024307, Aug 2019.

[WSP$^+$21] M. Weinert, M. Spieker, G. Potel, N. Tsoneva, M. Müscher, J. Wilhelmy, and A. Zilges. Microscopic structure of the low-energy electric dipole response of ^{120}Sn. *Phys. Rev. Lett.*, 127:242501, 2021.

[Yan87] Constantine Yannouleas. Zero-temperature second random phase approximation and its formal properties. *Phys. Rev. C*, 35:1159–1161, 1987.

[YBSZ21] M. J. Yang, C. L. Bai, H. Sagawa, and H. Q. Zhang. Effects of the skyrme tensor force on 0^+, 2^+, and 3^- states in ^{16}O and ^{40}Ca nuclei within the second random-phase approximation. *Phys. Rev. C*, 103:054308, 2021.

[YDG83] C. Yannouleas, M. Dworzecka, and J.J. Griffin. Microscopic nuclear dissipation: (ii). damping of collective states in subspaces which include 2p-2h states. *Nuclear Physics A*, 397(2):239–295, 1983.

A. EMPM original papers

A.1 A self-consistent study of multipole response in neutron-rich nuclei using a modified realistic potential

D. Bianco, F. Knapp, N. Lo Iudice, P. Veselý, F. Andreozzi, G. De Gregorio and A. Porrino

Journal of Physics G: Nuclear and Particle Physics 41 025109 (2014)

DOI:10.1088/0954-3899/41/2/025109

A.2 Upgraded formulation of the nuclear eigenvalue problem in a microscopic multiphonon basis

D. Bianco, F. Knapp, N. Lo Iudice, F. Andreozzi, and A. Porrino

Physical Review C 85, 014313 (2012)

DOI:10.1103/PhysRevC.85.014313

A.3 Dipole response in ^{132}Sn within a self-consistent multiphonon approach

F. Knapp, N. Lo Iudice, P. Veselý, F. Andreozzi, G. De Gregorio and A. Porrino

Physical Review C 90, 014310 (2014)

DOI:10.1103/PhysRevC.90.014310

A.4 Self-consistent quasiparticle formulation of a multiphonon method and its application to the neutron-rich ^{20}O nucleus

G. De Gregorio, F. Knapp, N. Lo Iudice and P. Veselý

Physical Review C 93, 044314 (2016)

DOI:10.1103/PhysRevC.93.044314

A.5 Ground-state correlations within a nonperturbative approach

G. De Gregorio, J. Herko, F. Knapp, N. Lo Iudice and P. Veselý

Physical Review C 95, 024306 (2017)

DOI:10.1103/PhysRevC.95.024306

A.6 Low- and high-energy spectroscopy of ^{17}O and ^{17}F within a microscopic multiphonon approach

G. De Gregorio, F. Knapp, N. Lo Iudice and P. Veselý

Physical Review C 95, 034327 (2017)

DOI:10.1103/PhysRevC.99.014316

A.7 Proper treatment of the Pauli principle in mirror nuclei within the microscopic particle(hole) -phonon scheme

G. De Gregorio, F. Knapp, N. Lo Iudice and P. Veselý

Physical Review C 101, 024308 (2020)

DOI:10.1103/PhysRevC.101.024308

A.8 Removal of the center of mass in nuclei and its effects on ^{4}He

G. De Gregorio, F. Knapp, N. Lo Iudice and P. Veselý

Physics Letters B 821, 136636 (2021)

DOI:10.1016/j.physletb.2021.136636

A.9 Spectroscopic properties of ^{4}He within a multiphonon approach

G. De Gregorio, F. Knapp, N. Lo Iudice and P. Veselý

Physical Review C 105, 024326 (2022)

DOI:10.1103/PhysRevC.105.024326

B. Shell model original papers

B.1 Matrix diagonalization algorithm and its applicability to the nuclear shell model

D. Bianco, F. Andreozzi, N. Lo Iudice, A. Porrino, and F. Knapp

Physical Review C 84, 024310 (2011)

DOI: 10.1103/PhysRevC.84.024310

B.2 Importance-sampling diagonalization algorithm for large-scale shell model calculations on N = 80 isotones

D. Bianco, F. Andreozzi, N. Lo Iudice, A. Porrino, and F. Knapp

Physical Review C 85, 034332 (2012)

DOI:10.1103/PhysRevC.85.034332

B.3 Mixed-symmetry states in Te isotopes within a large-scale shell model approach

D. Bianco, N. Lo Iudice, F. Andreozzi, A. Porrino, and F. Knapp

Physical Review C 86, 044325 (2012)

DOI:10.1103/PhysRevC.86.044325

B.4 Importance basis truncation in the symmetry-adapted no-core shell model

F. Knapp, T. Dytrych, D. Langr and T. Oberhuber

Acta Physica Polonica B 50, 541 (2019)

DOI:10.5506/APhysPolB.50.541